

## ***Electronic Supplementary Information***

### **(Z)-3-(Quinolin-2-ylmethylene)-3,4-dihydroquinoxalin-2(1H)-one derivatives: AIE--active compounds with pronounced effects of ESIPT and TICT**

Qi-Chao Yao, Xiao-Lin Lu, Min Xia\*

Department of Chemistry, Zhejiang Sci-Tech University, Hangzhou 310018, P. R. China

E-mail: [xiamin@zstu.edu.cn](mailto:xiamin@zstu.edu.cn)

#### **Instruments and measurements**

All the reagents used were analytically pure and some chemicals were further purified by recrystallization or distillation. Melting points were determined by an OptiMelt automated melting point system. The  $^1\text{H}$  NMR (400 MHz) and  $^{13}\text{C}$  NMR (100 MHz) spectra were obtained on a Bruker Avance II DMX400 spectrometer using DMSO-d<sub>6</sub> as the solvent and tetramethylsilane as the internal standard. The absorption spectra were measured on a Shimadzu UV 2501(PC)S UV–Vis spectrometer and the fluorescence spectra were acquired on a Perkin-Elmer LS55 spectrophotometer. Quantum yields in THF were measured with quinine sulfate in 0.05M H<sub>2</sub>SO<sub>4</sub> aqueous solution ( $\Phi_f=0.55$ ) or fluorescein in 0.1N NaOH aqueous solution ( $\Phi_f=0.91$ ) as the reference. The mass spectra were recorded on a HP 1110 mass spectrometer. Particle size is determined on a Beckman Coulter particle analyzer with 10  $\mu\text{M}$  aggregate in THF/H<sub>2</sub>O mixture (10 : 90, v/v) at 25 °C.

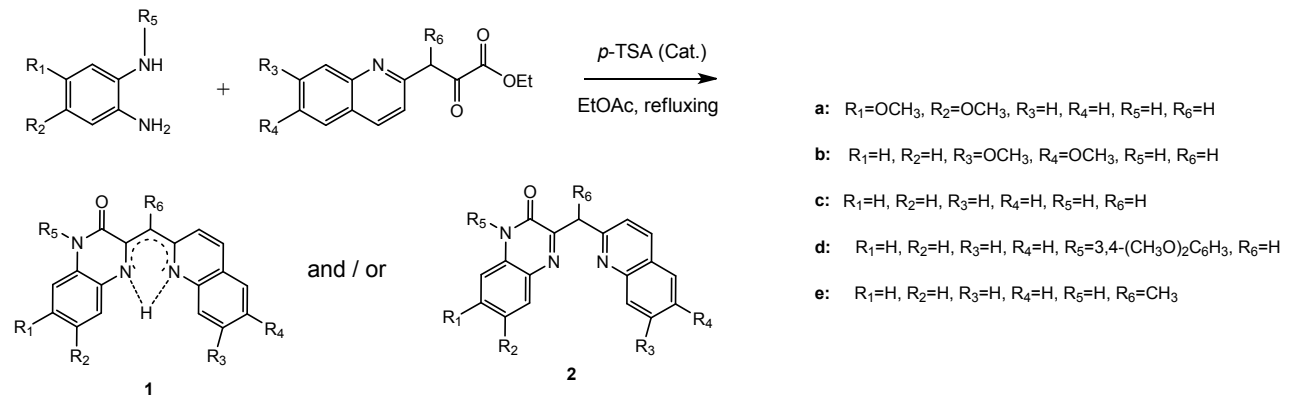
#### **Computational details**

The gas-phase geometries of the concerned complexes were optimized without any symmetry restrictions in singlet ground state using the density functional theory (DFT) method at the B3LYP level [1]. The 6–31G (d, p) basis set was selected for all the elements. The vibration frequency calculations were performed to ensure that the optimized geometries represented the local minima on the ground-state potential energy surface. All the calculations were carried out with the Gaussian 09 program package in the aid of the GaussView visualization program [2].

The potential energy curves (PECs) of the ground state intramolecular proton transfer were calculated with the energies of the B3LYP/6-31G (d, p) fully optimized structures at the fixed N<sub>1</sub>–H distances over the 0.8–2.2 Å. The PECs of the corresponding excited state intramolecular proton transfer were obtained by adding the TD-DFT/ B3LYP/6-31G (d, p) calculated vertical transition energy of the first singlet excited state to the energy

of the ground state. The PECs of the ground state intramolecular torsion were calculated with energies of the B3LYP/6-31G (d, p) fully optimized structures at the fixed C<sub>3</sub>-C<sub>4</sub>-C<sub>5</sub>-N<sub>2</sub> angle over the -90~270° range for **1c** and -90~90° for **1a** and **1b**. The PECs of the corresponding excited state intramolecular torsion were obtained by adding the TD-DFT/B3LYP/6-31G (d, p) calculated vertical transition energy of the first singlet excited state to the energy of the ground state. The solvent effect on the ground and the first singlet excited state were executed with the polarizable continuum model (PCM)<sup>[3]</sup>.

### General procedure for preparation of compound **1a-d**, **2e**, **3a** and **3a-Bn**



At room temperature, *o*-phenylenediamine (1 mmol), ethyl 2-oxo-3-(quinolin-2-yl)propanoate (1 mmol) or ethyl 2-oxo-3-(quinolin-2-yl)butanoate (1 mmol) and *p*-toluenesulfonic acid (0.1 mmol) are mixed in ethyl acetate (5 mL). The resulted mixture is refluxed for 24h to offer the product as the solid. After the filtration, the solid is washed by ethanol and ether for several times followed by the recrystallization in the EtOH/THF mixture.

**1a** and **2a** mixture: 75% overall yield, dark red powder, m.p. 215.6°C-216.3; EI-MS (70 eV) *m/z* (%) 347(M<sup>+</sup>, 100), 332(58), 319(15), 304(23), 275(15), 261(18), 168(15), 143(42), 128(18).

**1a:** <sup>1</sup>H NMR(400MHz, DMSO-d<sub>6</sub>) δ 3.75(s, 3H), 3.89(s, 3H), 6.26(s, 1H), 6.71(s, 1H), 7.14(s, 1H), 7.31(d, *J*=8 Hz, 1H), 7.39(t, *J*=8 Hz, 1H), 7.65-7.70(m, 1H), 7.72-7.76(m, 1H), 7.97 (d, *J*=8 Hz, 1H), 8.12(d, *J*=8 Hz, 1H), 11.47(s, 1H), 13.71(s, 1H); <sup>13</sup>C NMR(100MHz, DMSO-d<sub>6</sub>) δ 55.80, 56.21, 91.82, 99.34, 102.08, 119.78, 121.28, 123.70, 124.33, 124.40, 124.65, 127.50, 129.88, 134.72, 140.87, 144.08, 145.15, 145.58, 154.77, 156.36.

**2a:** <sup>1</sup>H NMR(400MHz, DMSO-d<sub>6</sub>) δ 3.78(s, 3H), 3.83(s, 3H), 4.44(s, 2H), 6.79(s, 1H), 7.17(s, 1H), 7.51-7.57(m, 2H), 7.71(d, *J*=8 Hz, 1H), 7.89(d, *J*=8 Hz, 1H), 7.94(d, *J*=8 Hz, 1H), 8.28 (d, *J*=8 Hz, 1H), 12.30(s, 1H); <sup>13</sup>C NMR(100MHz, DMSO-d<sub>6</sub>) δ 42.41, 55.71, 55.75, 96.92, 109.41, 122.42, 125.97, 126.60, 126.95, 127.80, 128.44, 129.41, 136.14, 145.72, 147.22, 151.09, 154.61, 155.95, 159.02.

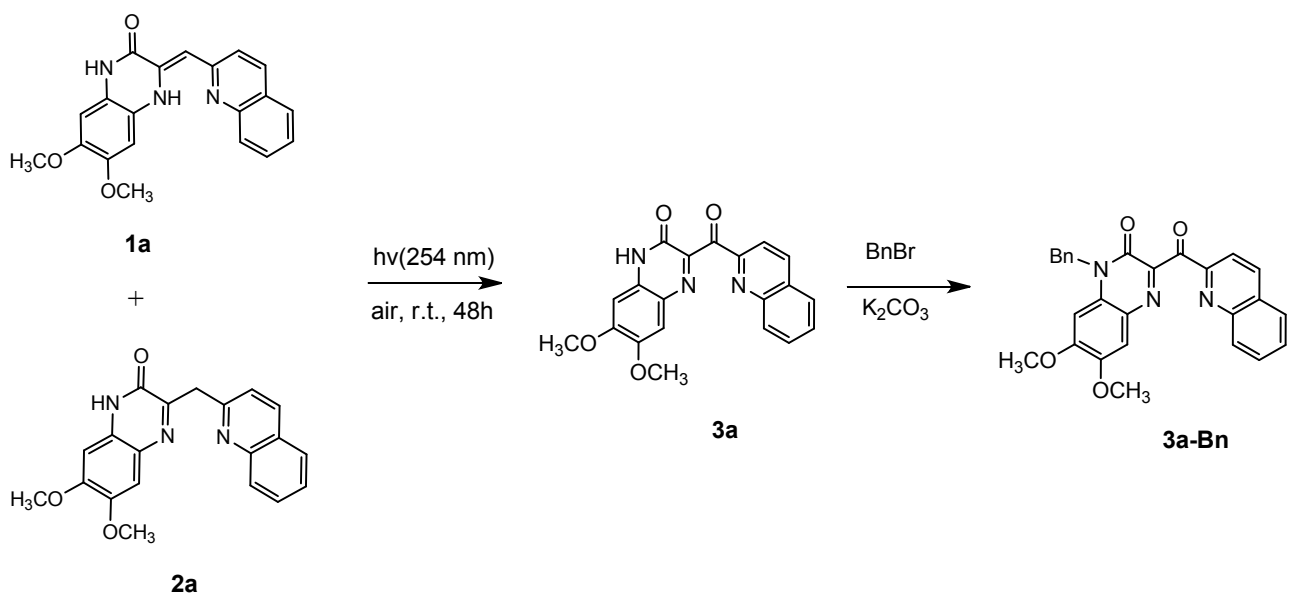
**1b:** 83% yield, orange powder, m.p. 256.3-256.9 °C; EI-MS (70 eV) *m/z* (%) 347(M<sup>+</sup>, 100), 332(13), 303(15), 275(15), 203(8), 173(8), 156(10), 90(10); <sup>1</sup>H NMR(400MHz, DMSO-d<sub>6</sub>) δ 3.91(s, 3H), 4.04(s, 3H), 6.35(s, 1H), 6.93(d, *J*=8 Hz, 1H), 7.05(s, 1H), 7.29(s, 1H), 7.33(d, *J*=8 Hz, 1H), 7.44(d, *J*=8 Hz, 1H), 7.57(s, 1H), 8.06(d, *J*=8

Hz, 1H), 11.33(s, 1H), 13.20(s, 1H);  $^{13}\text{C}$  NMR(100MHz, DMSO-d<sub>6</sub>)  $\delta$  55.59, 55.89, 95.67, 105.98, 106.92, 114.63, 114.90, 120.64, 120.93, 121.12, 123.21, 125.30, 126.41, 134.34, 135.12, 143.03, 148.62, 152.38, 155.07, 157.48.

**1c:** 88% yield, red powder, m.p. 245.5-246.2°C; EI-MS (70 eV)  $m/z$  (%) 287(M<sup>+</sup>, 100), 258(91), 168(10), 143(23), 129(25), 115(10), 101(8), 90(12), 77(10);  $^1\text{H}$  NMR(400MHz, DMSO-d<sub>6</sub>)  $\delta$  6.40(s, 1H), 6.99(t,  $J=8$  Hz, 1H), 7.06-7.11(m, 2H), 7.44-7.51(m, 3H), 7.75(t,  $J=8$  Hz, 1H), 7.87(d,  $J=8$  Hz, 1H), 8.20(dd,  $J_1=8$  Hz,  $J_2=4$  Hz, 2H), 11.50(s, 1H), 13.73(s, 1H);  $^{13}\text{C}$  NMR(100MHz, DMSO-d<sub>6</sub>)  $\delta$  94.35, 115.00, 115.21, 121.55, 123.31, 125.09, 125.14, 125.68, 126.35, 126.83, 127.55, 129.81, 135.67, 137.53, 145.74, 157.00, 157.05.

**1d:** 85% yield, red powder, m.p. 263.4-263.9°C; EI-MS (70 eV)  $m/z$  (%) 423(M<sup>+</sup>, 100), 395(25), 308(20), 258(20), 211(22), 182(22), 168(32), 140(35), 128(57), 115(35), 79(23);  $^1\text{H}$  NMR(400MHz, DMSO-d<sub>6</sub>)  $\delta$  3.76(s, 3H), 3.87(s, 3H), 6.38(d,  $J=8$  Hz, 1H), 6.46(s, 1H), 6.90(t,  $J=8$  Hz, 1H), 6.95(d,  $J=8$  Hz, 1H), 7.05(s, 1H), 7.12-7.18(m, 2H), 7.49-7.55(m, 3H), 7.76(t,  $J=8$  Hz, 1H), 7.87(d,  $J=8$  Hz, 1H), 8.19(d,  $J=8$  Hz, 1H), 8.23(d,  $J=8$  Hz, 1H), 13.99(s, 1H);  $^{13}\text{C}$  NMR(100MHz, DMSO-d<sub>6</sub>)  $\delta$  55.66, 55.74, 94.87, 112.27, 112.33, 115.60, 115.78, 120.77, 121.43, 123.46, 123.68, 125.17, 126.67, 126.91, 127.61, 129.00, 129.43, 129.92, 135.73, 137.55, 145.51, 148.88, 149.78, 156.74, 156.86.

**2e:** 72% yield, white powder, m.p. 164.7-165.4°C; EI-MS (70 eV)  $m/z$  (%) 301(M<sup>+</sup>, 38), 286(100), 272(12), 156(50), 145(18), 128(40), 101(15), 90(18), 77(15);  $^1\text{H}$  NMR(400MHz, DMSO-d<sub>6</sub>)  $\delta$  1.68(d,  $J=8$  Hz, 3H), 4.93(q,  $J=8$  Hz, 1H), 7.10 (m, 1H), 7.50-7.59(m, 3H), 7.67(t,  $J=8$  Hz, 1H), 7.82(t,  $J=8$  Hz, 2H), 7.93(d,  $J=8$  Hz, 1H), 8.29(d,  $J=8$  Hz, 1H), 12.3(s, 1H);  $^{13}\text{C}$  NMR(100MHz, DMSO-d<sub>6</sub>)  $\delta$  17.98, 44.41, 115.20, 121.32, 123.05, 125.81, 126.54, 127.62, 128.45, 128.48, 129.21, 129.65, 131.48, 131.84, 136.25, 146.97, 154.21, 155.08, 162.37, 163.34.



At room temperature, the solution of **1a/2a** mixture (1 mmol) in THF (2 mL) is irradiated at 254 nm under a low pressure mercury lamp for 48h. The solution is concentrated on a rotating evaporator and the residue is isolated by column chromatography on silica gel with petroleum ether (60-90°C)/acetone (3:1) as the eluent. The product **3a** is the yellow powder in 88% yield.

**3a:** m.p. 185.2 °C (decomp.); EI-MS (70 eV) *m/z* (%) 361(M<sup>+</sup>, 52), 332(25), 204(18), 177(20), 150(18), 129(100), 120 (16), 101(31), 77(21); <sup>1</sup>H NMR(400MHz, DMSO-d<sub>6</sub>) δ 3.84(s, 3H), 3.92(s, 3H), 6.91(s, 1H), 7.39(s, 1H), 7.78(t, *J*=8 Hz, 1H), 7.83(t, *J*=8 Hz, 1H), 7.98(d, *J*=8 Hz, 1H), 8.15(d, *J*=8 Hz, 1H), 8.20(d, *J*=8 Hz, 1H), 8.68(d, *J*=8 Hz, 1H), 12.72(s, 1H).

At room temperature, potassium carbonate (2 mmol) is added to the solution of **3a** (1 mmol) and benzyl bromide (1.2 mmol) in acetone (2 mL), the resulted mixture is refluxing for 24h. After cooling to room temperature, the mixture is filtrated and the filtrate is concentrated on a rotating evaporator. The residue is isolated by column chromatography on silica gel with petroleum ether (60-90°C)/acetone (2:1) as the eluent. The product **3a-Bn** is the orange powder in 81% yield.

**3a-Bn:** m.p. 217.3-218.6°C; EI-MS (70 eV) *m/z* (%) 451(M<sup>+</sup>, 43), 360 (95), 332(83), 316(20), 288(20), 218(22), 128(100), 101(30), 91(100), 77(15); <sup>1</sup>H NMR(400MHz, DMSO-d<sub>6</sub>) δ 3.84(s, 3H), 3.86(s, 3H), 5.61(s, 2H), 7.08(s, 1H), 7.31-7.35(m, 1H), 7.40-7.42(m, 4H), 7.47(s, 1H), 7.79(td, *J*= 8 Hz, *J*= 1.6 Hz, 1H), 7.89(td, *J*= 8 Hz, *J*= 1.6 Hz, 1H), 7.94(d, *J*= 8 Hz, 1H), 8.14(d, *J*=8 Hz, 1H), 8.25(d, *J*=8 Hz, 1H), 8.70(d, *J*=8 Hz, 1H); <sup>13</sup>C NMR (100MHz, DMSO-d<sub>6</sub>) δ 44.23, 55.93, 56.23, 97.79, 111.02, 118.17, 126.77, 127.08, 127.62, 128.27, 128.78, 129.34, 129.49, 129.64, 130.89, 135.61, 138.24, 146.28, 146.45, 152.27, 152.69, 152.88, 153.47, 193.68.

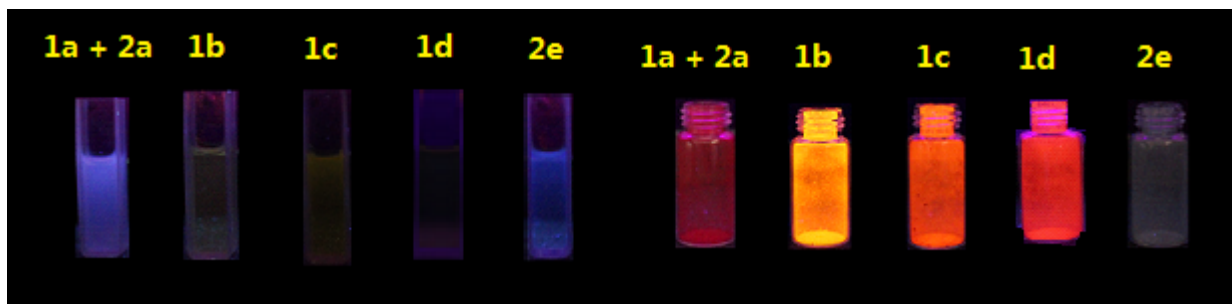
**Table S1** The difference of Gibbs free energy between the tautomers based on the calculations at DFT/B3LYP/PCM/6-31G(d,p) method in DMSO at 25°C and 1 atm <sup>a</sup>

Compd	$\Delta G_1$ (KJ/mol) <sup>b</sup>	$\Delta G_2$ (KJ/mol) <sup>c</sup>	Cal. ratio <sup>d</sup> of		Exp. ratio <sup>e</sup> of		Cal. ratio <sup>d</sup> of	
			<b>1</b>	<b>2</b>	<b>1</b>	<b>2</b>	<b>1N</b>	<b>1T</b>
<b>a</b>	3.217	2.884	3.2	:	1	3.3	:	1
<b>b</b>	7.003	17.572	1350	:	1	> 50	:	1
<b>c</b>	4.452	17.543	1335	:	1	> 50	:	1
<b>d</b>	5.593	9.989	57	:	1	> 50	:	1
<b>e</b>	--	-5.849	1	:	11	< 1	:	50

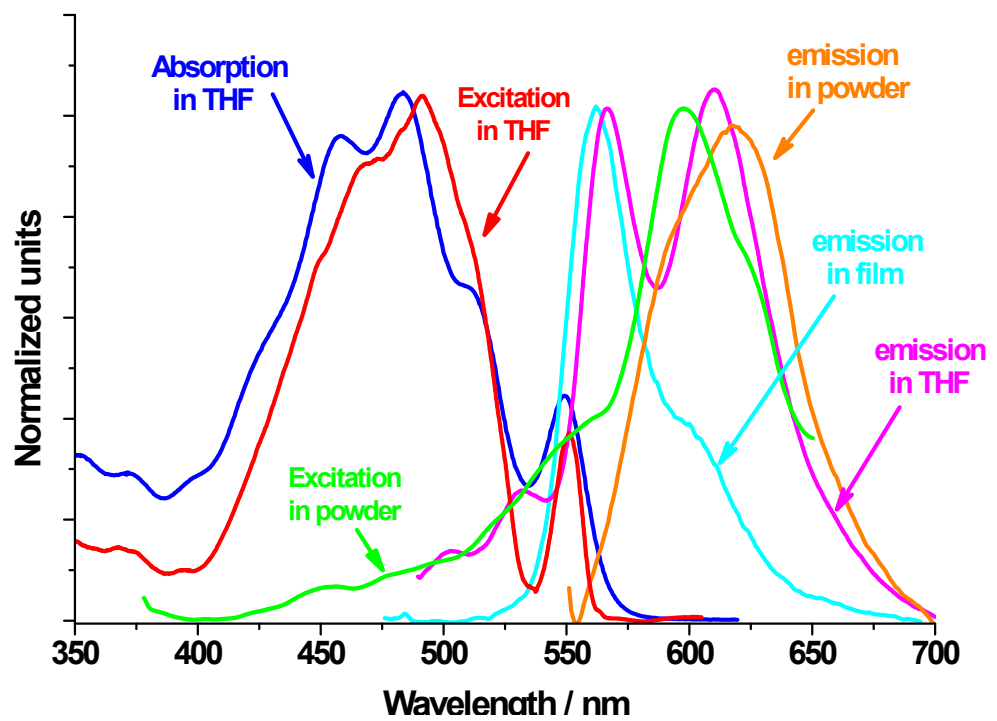
<sup>a</sup> Taking the Gibbs free energy of **1N** isomer as the reference in a given product;

<sup>b</sup> $\Delta G_1 = G_{IT} - G_{IN}$ ; <sup>c</sup> $\Delta G_2 = G_2 - G_{IN}$ ;

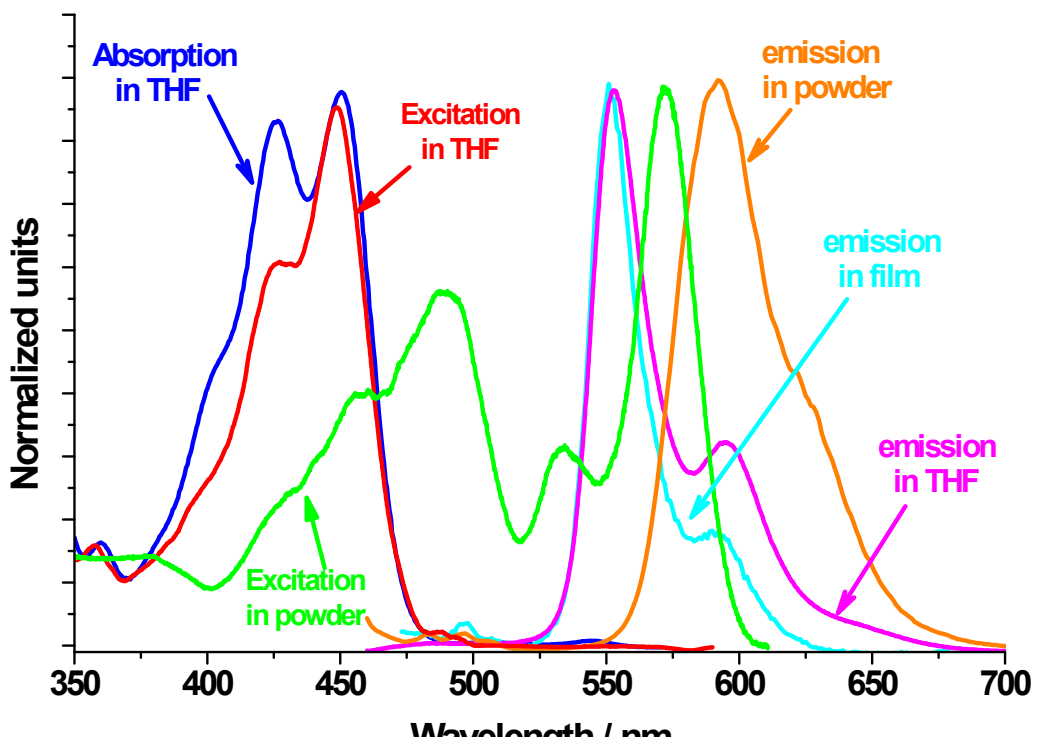
<sup>d</sup> Estimated by the  $\Delta G = -RT \ln K$  equation; <sup>e</sup> determined by the <sup>1</sup>H NMR



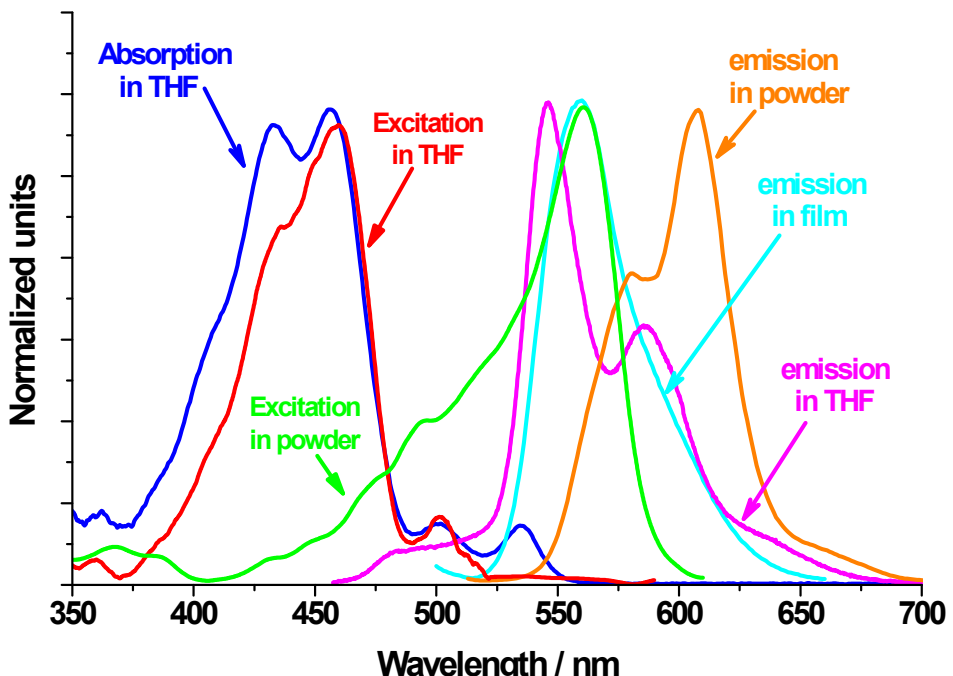
**Fig. S1** Photos of compounds in THF solution and coated on the inner wall of bottles under an ultraviolet lamp at 365 nm



**Fig. S2** The normalized absorption, excitation ( $\lambda_{\text{em}}$  at 615 nm) and emission ( $\lambda_{\text{ex}}$  at 480 nm) spectra of **1a** in THF solution ( $1 \times 10^{-4}$  M), PMMA film and solid state



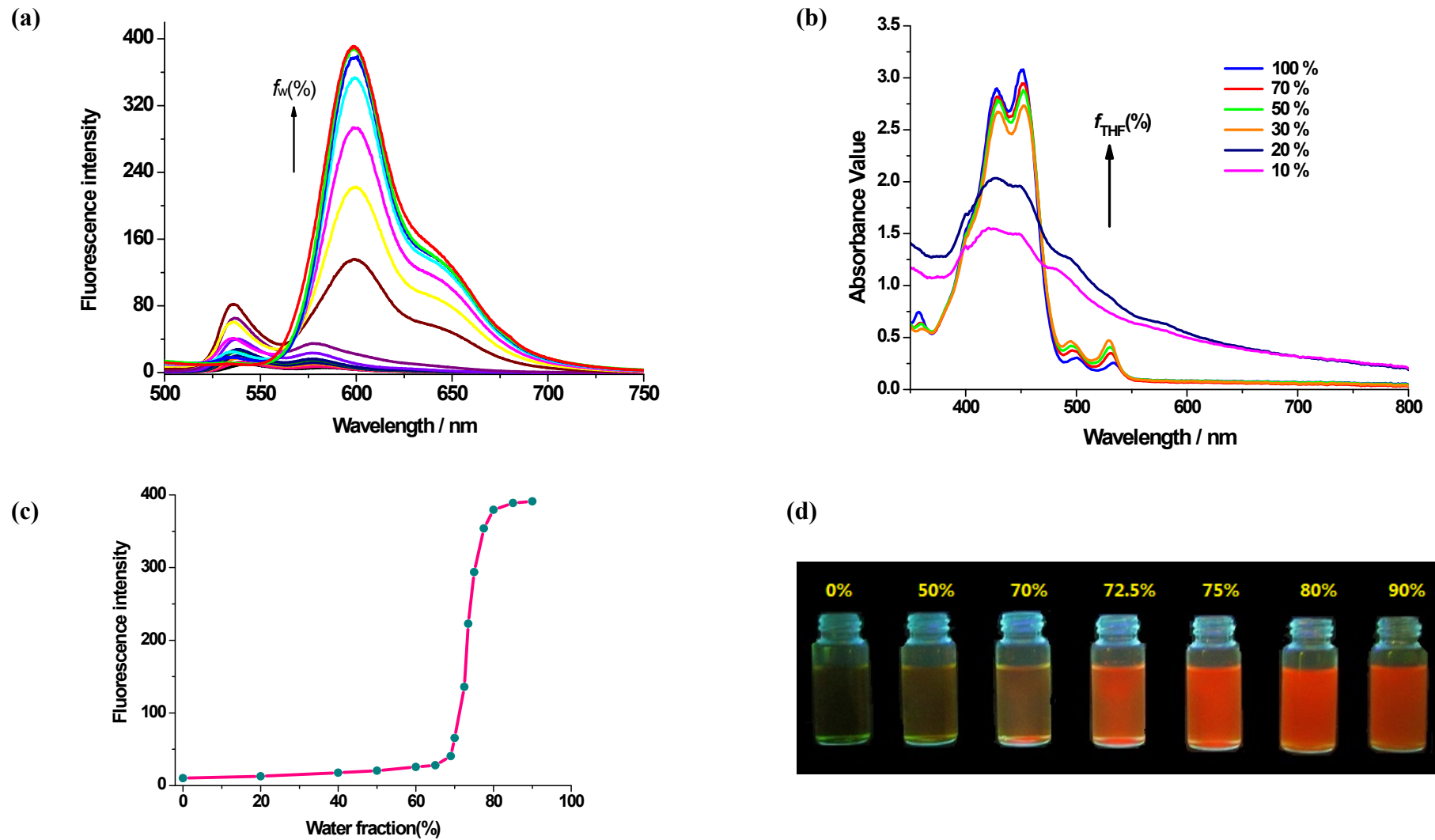
**Fig. S3** The normalized absorption, excitation ( $\lambda_{\text{em}}$  at 600 nm) and emission ( $\lambda_{\text{ex}}$  at 450 nm) spectra of **1b** in THF solution ( $1 \times 10^{-4}$  M), PMMA film and solid state



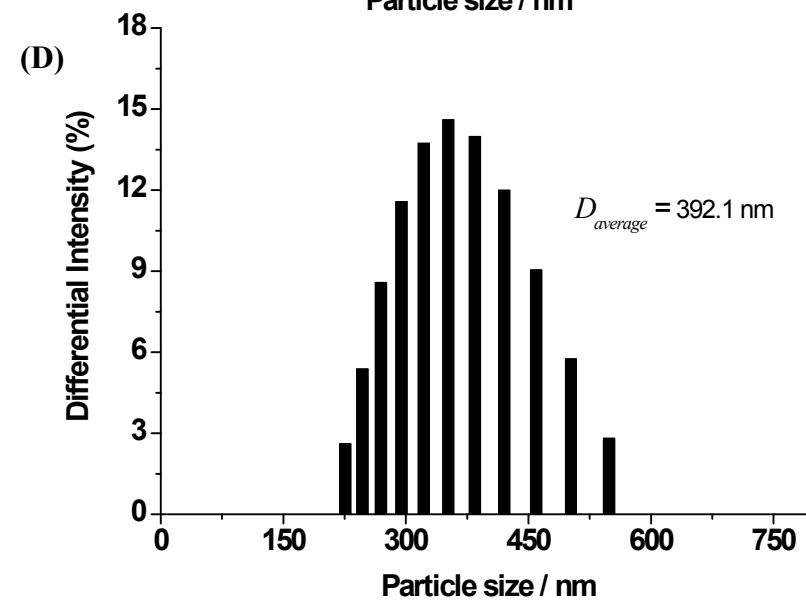
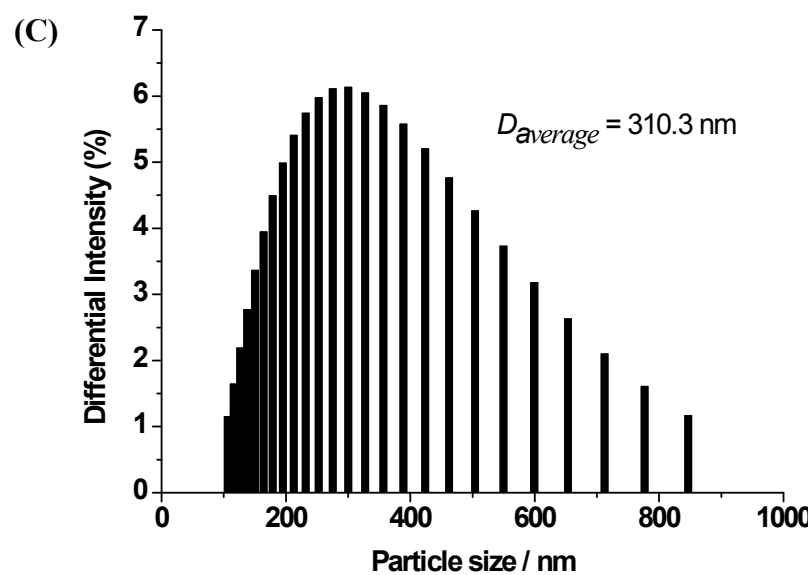
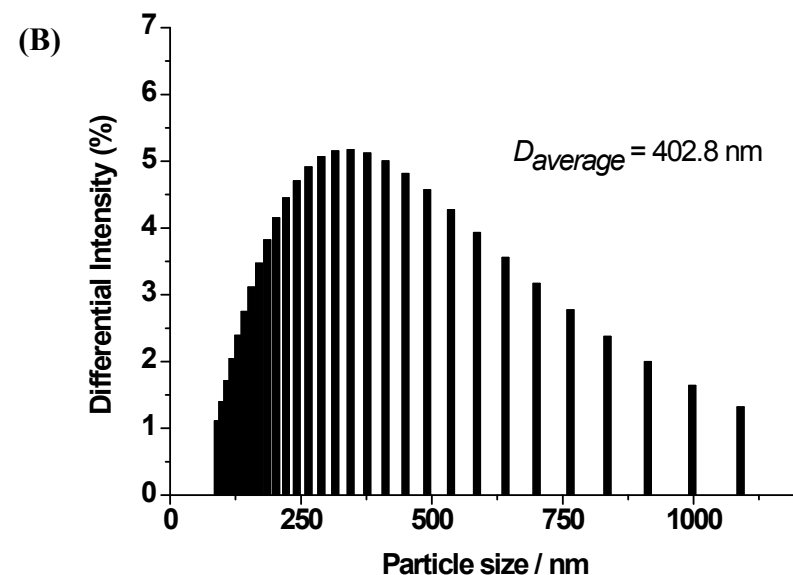
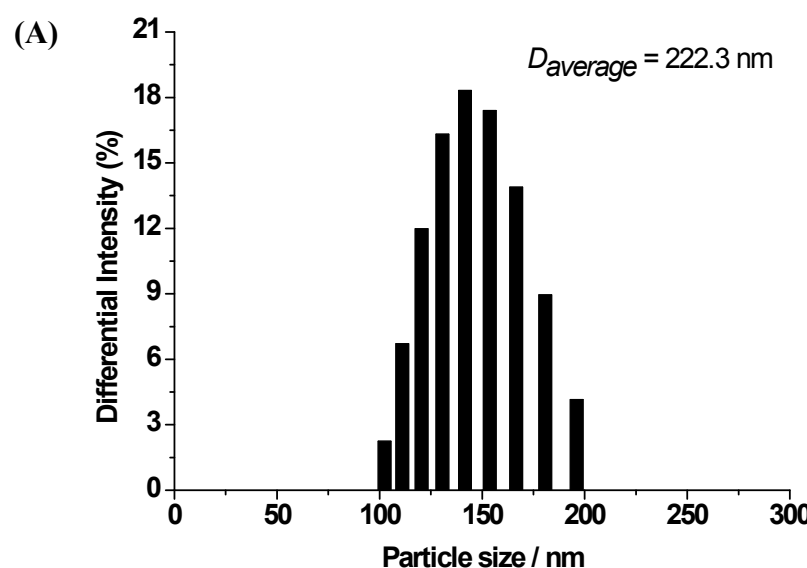
**Fig. S4** The normalized absorption, excitation ( $\lambda_{\text{em}}$  at 600 nm) and emission ( $\lambda_{\text{ex}}$  at 455 nm) spectra of **1d** in THF solution ( $1 \times 10^{-4}$  M), PMMA film and solid state



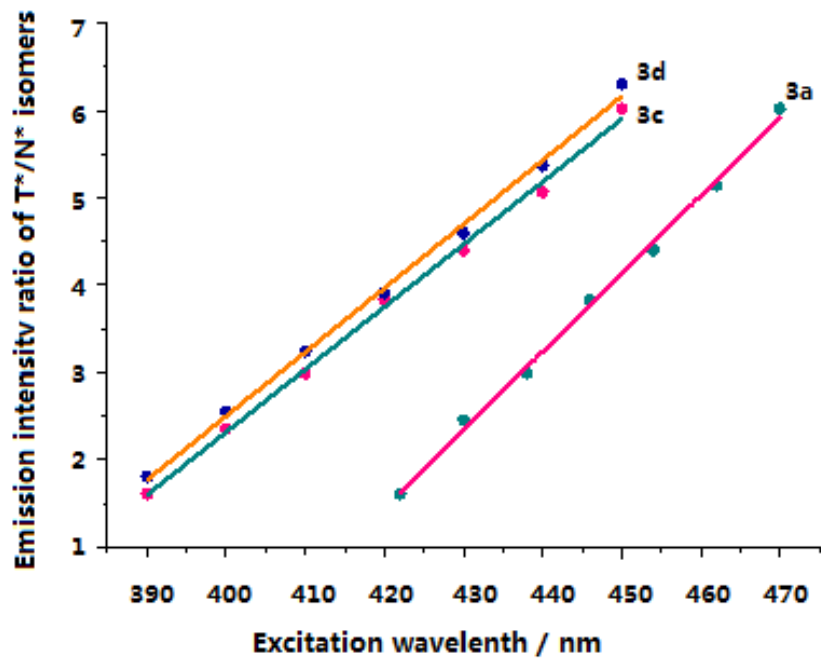
**Fig. S5** The normalized absorption and emission ( $\lambda_{\text{ex}}$  at 317 nm) spectra of **2e**



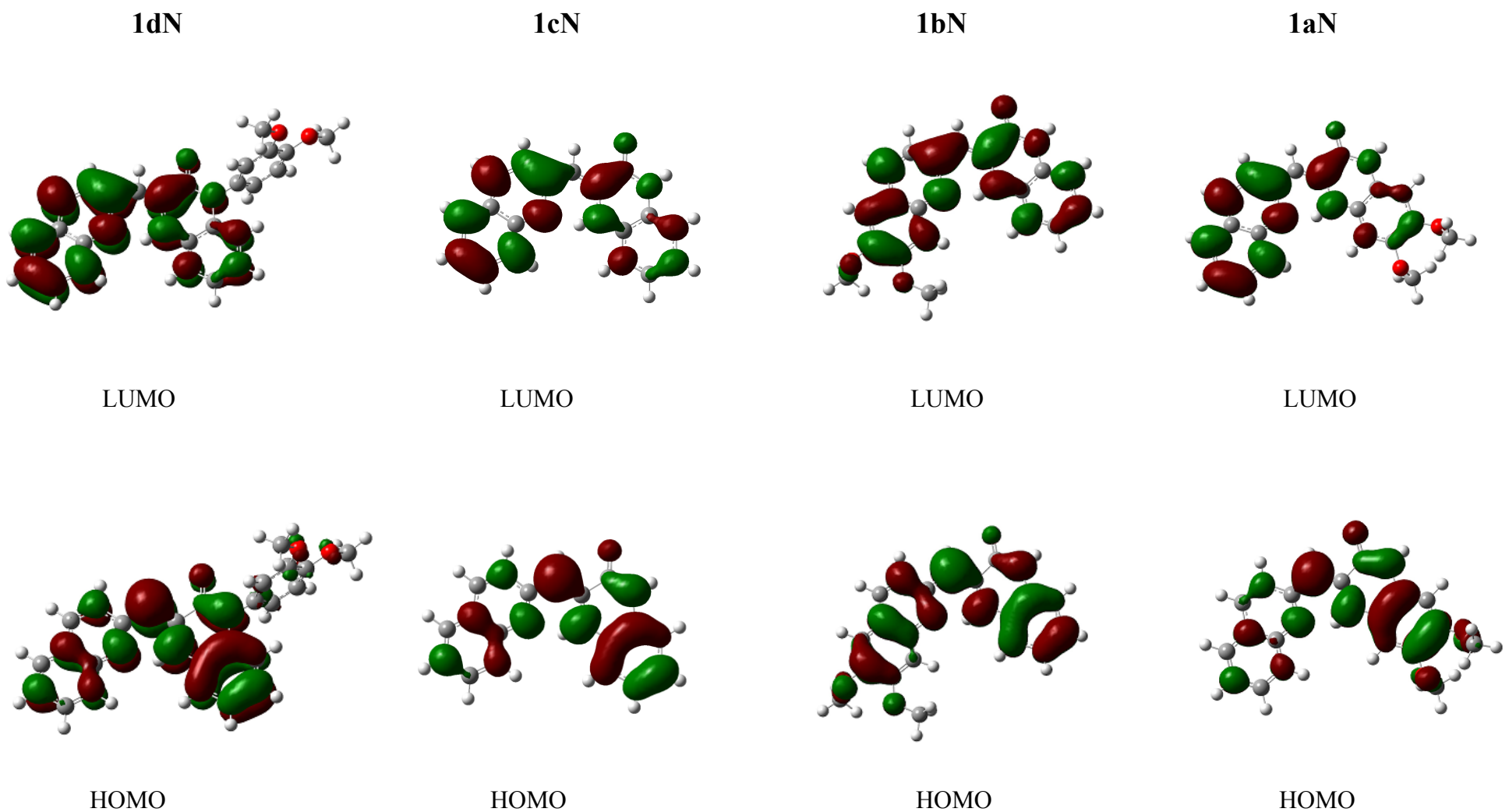
**Fig. S6** (a) Fluorescence (excited at 450 nm) and (b) absorption spectra of **1c** in  $1 \times 10^{-4}$  M THF/H<sub>2</sub>O mixture with varied water content; (c) fluorescence intensity of **1c** depending on water fraction ( $f_w$  %) in H<sub>2</sub>O/THF mixture; (d) photos under a hand-held ultraviolet lamp at 365 nm of **1c** with varied volumetric fractions of water in THF.



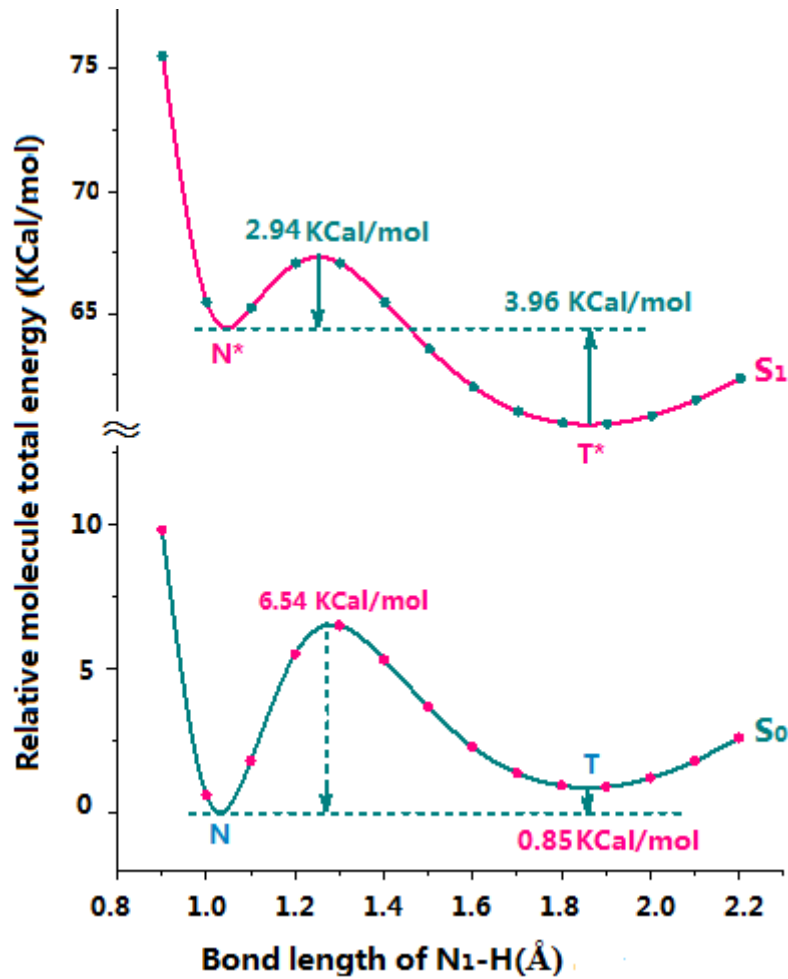
**Fig. S7** Size distribution by DLS of **1a** (A), **1b** (B), **1c** (C) and **1d**(D) aggregates ( $10 \mu\text{M}$ ) in THF/H<sub>2</sub>O (10:90, v/v) mixture solution



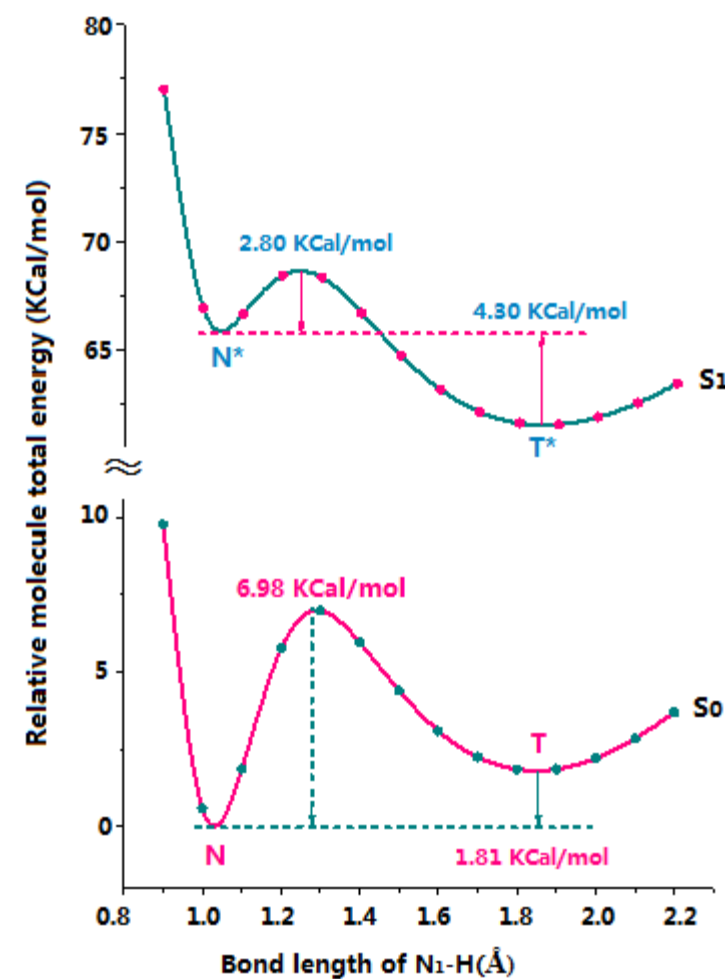
**Fig. S8** Emission intensity ratio of  $T^*/N^*$  isomers in **1a**, **1c** and **1d** ( $2 \times 10^{-5}$  M in THF) with varied excitation wavelength



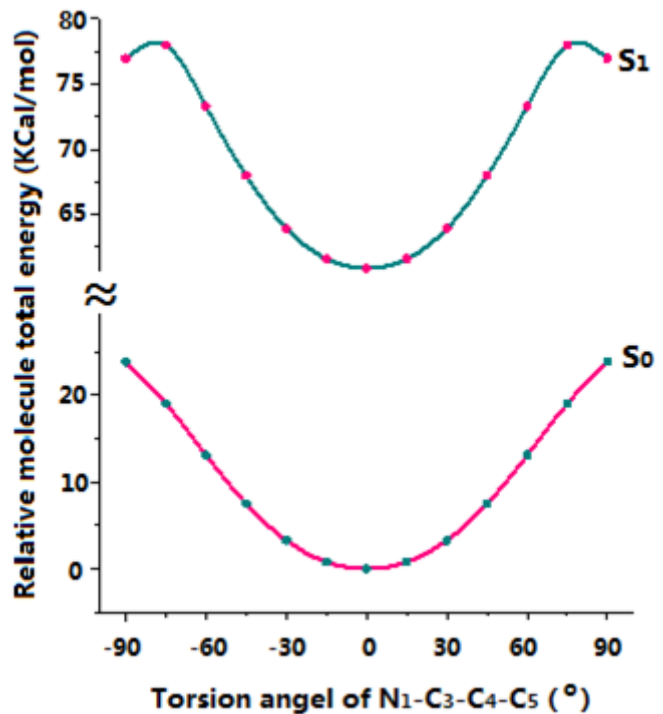
**Fig. S9** HOMOs and LUMOs of N-isomers in **1a-d**



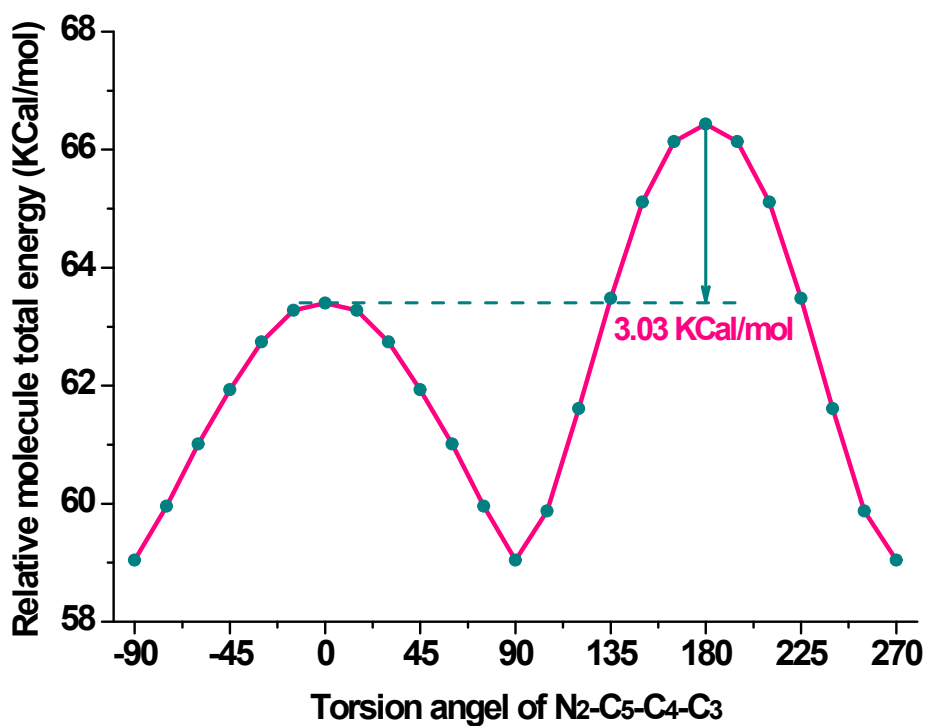
**Fig. S10** Relative molecule total energy with varied bond length of N<sub>1</sub>-H in **1aN** by TD-DFT calculations at B3LYP/PCM/6-31G(d,p) level in THF.



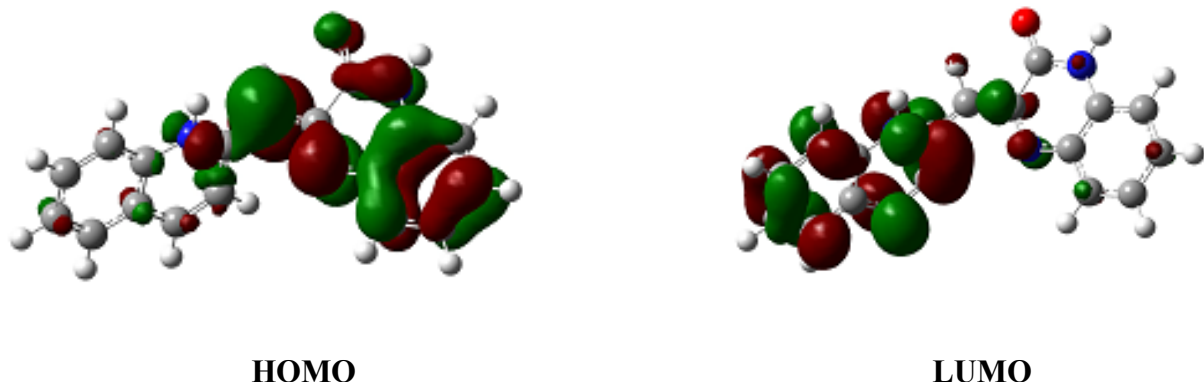
**Fig. S11** Relative molecule total energy with varied bond length of N<sub>1</sub>-H in **1bN** by TD-DFT calculations at B3LYP/PCM/6-31G(d,p) level in THF



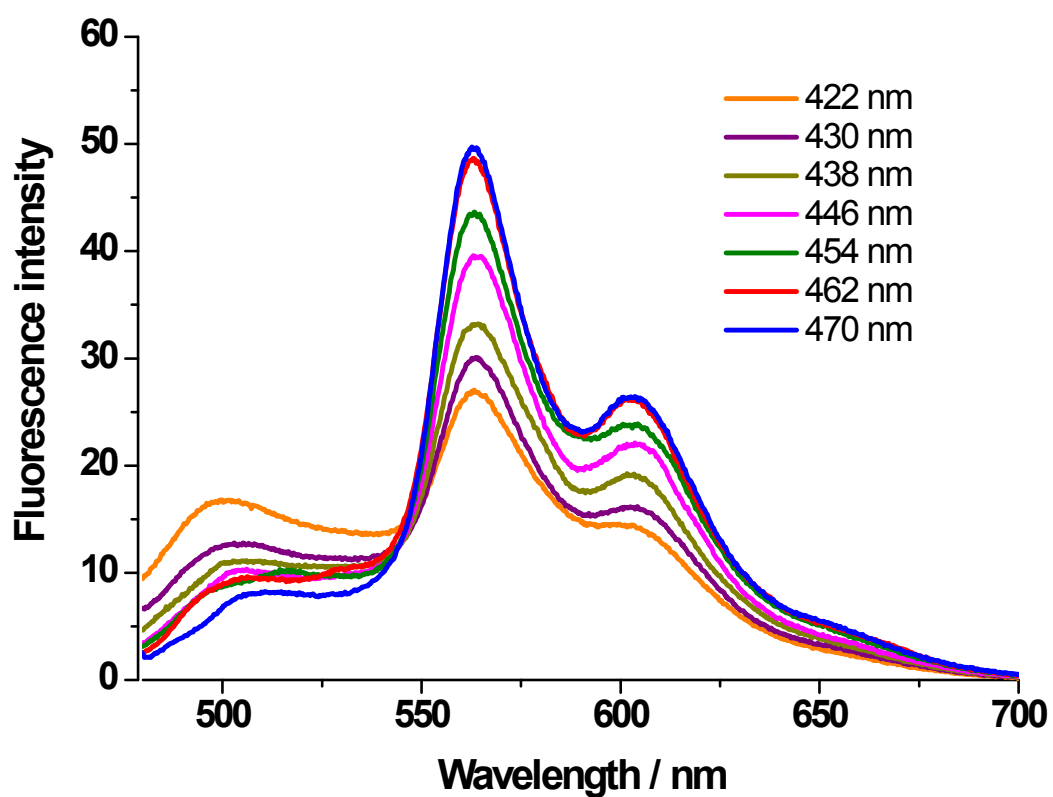
**Fig. S12** Relative molecule total energy with varied torsion angle of  $N_1\text{-}C_3\text{-}C_4\text{-}C_5$  in **1cT<sup>\*</sup>** by TD-DFT calculations at B3LYP/PCM/6-31G(d,p) level in THF



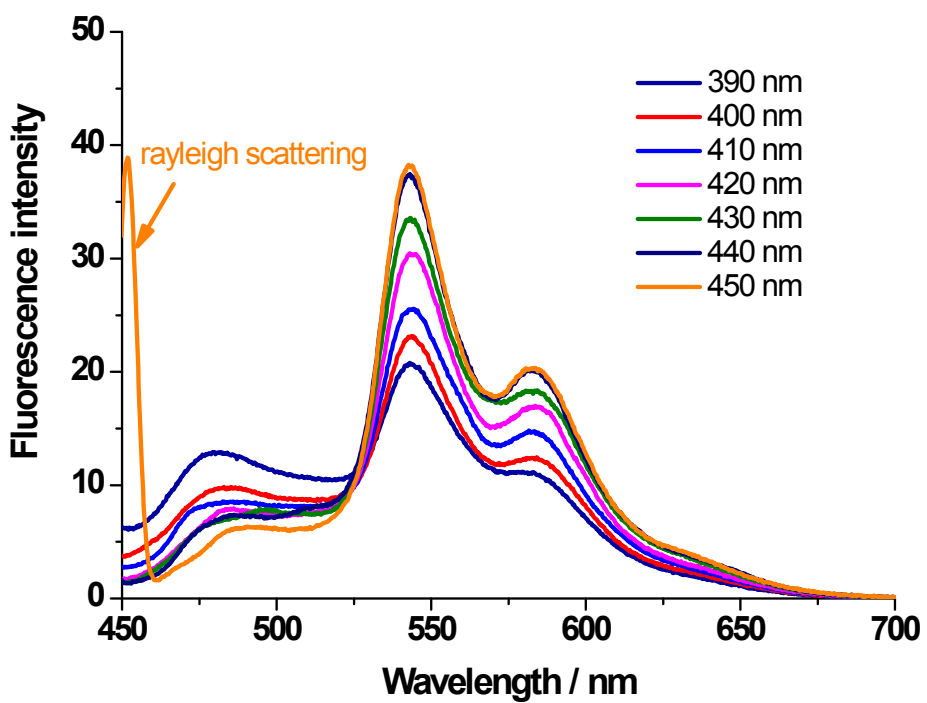
**Fig. S13** Relative molecule total energy with varied torsion angle of  $N_2\text{-}C_5\text{-}C_4\text{-}C_3$  in **1cT<sup>\*</sup>** by TD-DFT calculations at B3LYP/PCM/6-31G(d,p) level in THF



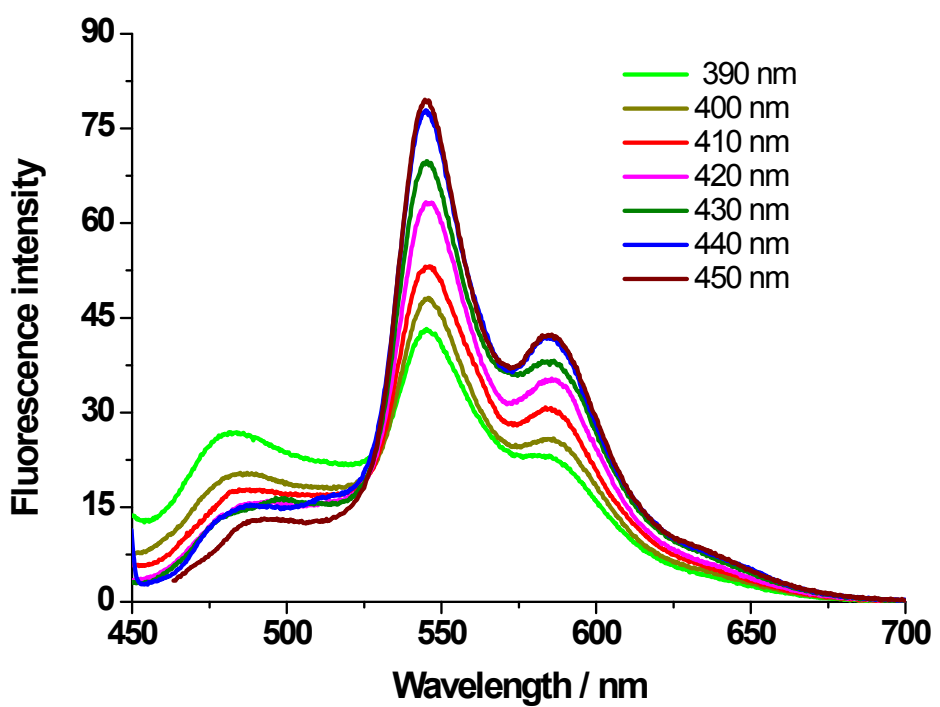
**Fig. S14** HOMO and LUMO of **1cT\*** in TICT state ( $90^\circ$  torsion angle of N<sub>2</sub>-C<sub>5</sub>-C<sub>4</sub>-C<sub>3</sub>)



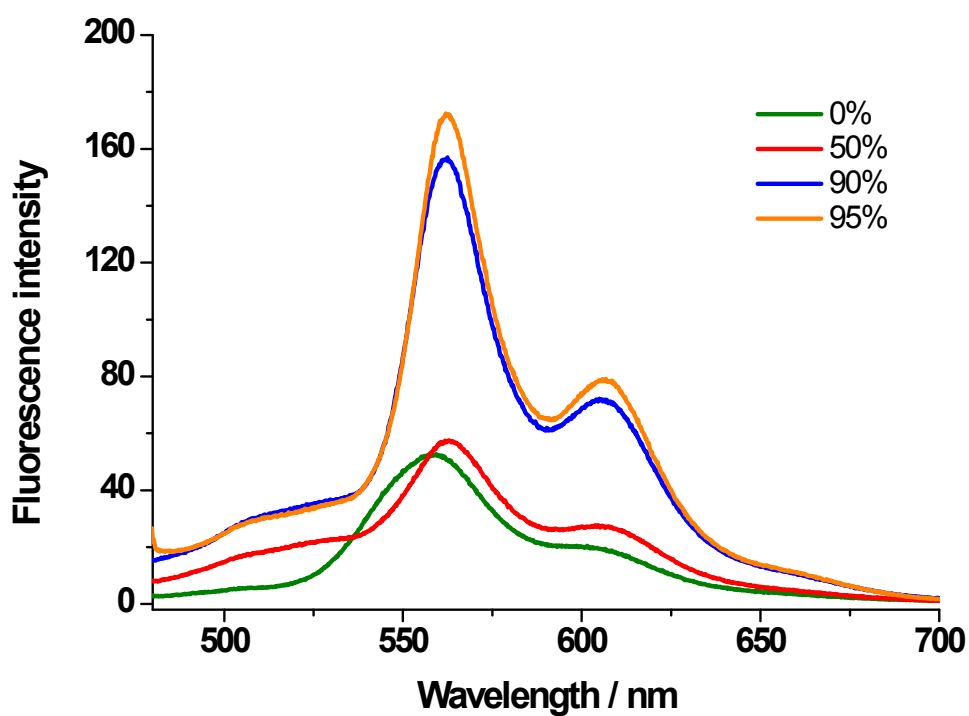
**Fig. S15** Emission spectra of **1a** ( $2 \times 10^{-5}$  M in THF) with varied excitation wavelength



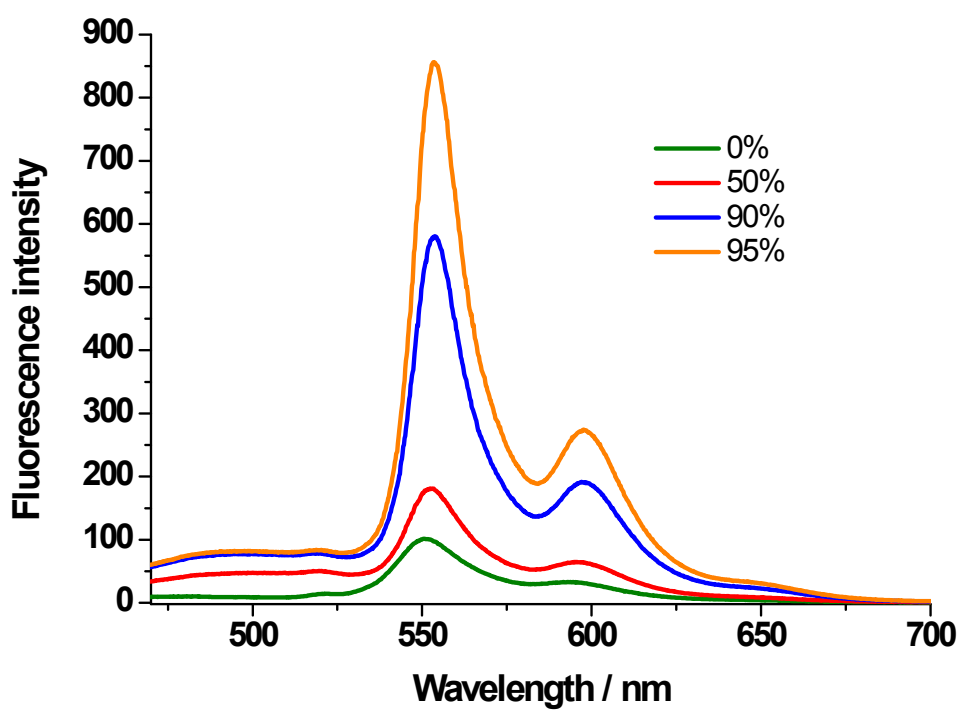
**Fig. S16** Emission spectra of **1c** (2×10<sup>-5</sup> M in THF) with varied excitation wavelength



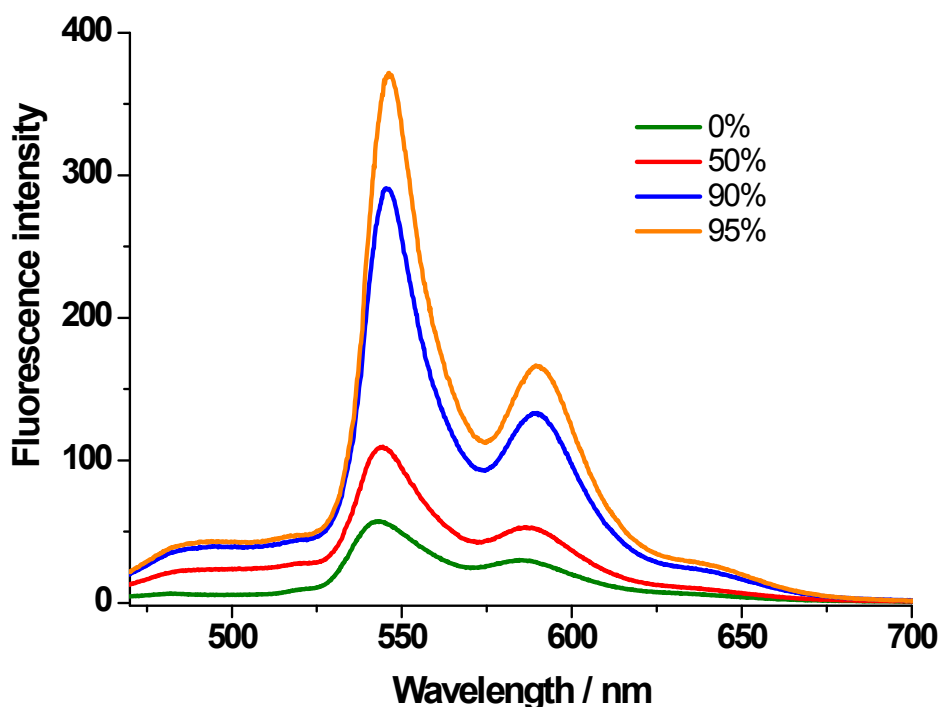
**Fig. S17** Emission spectra of **1d** (2×10<sup>-5</sup> M in THF) with varied excitation wavelength



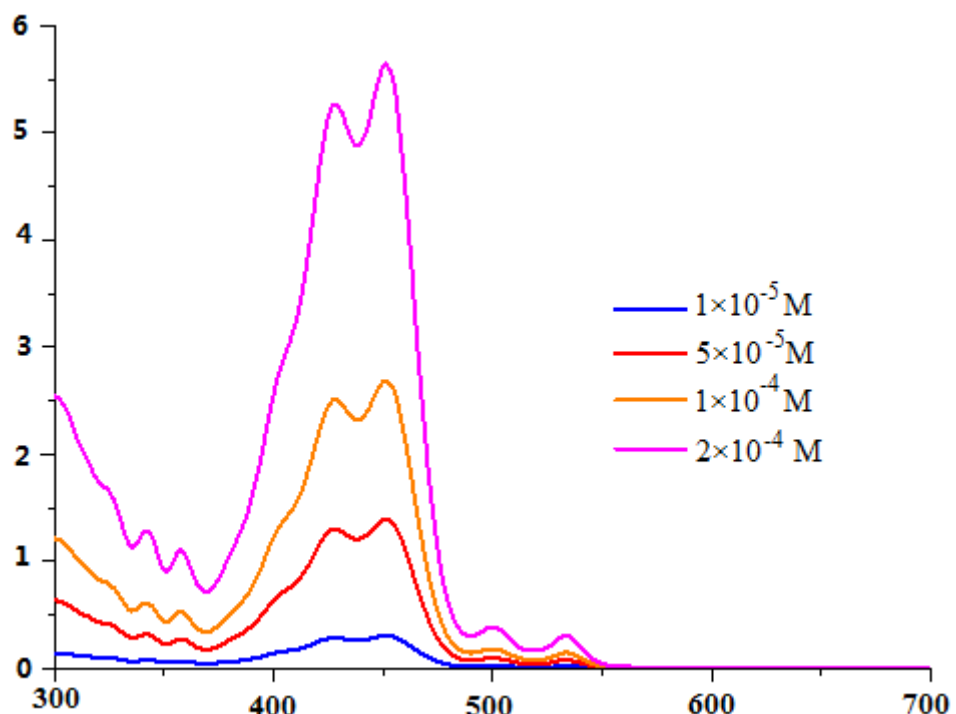
**Fig. S18** Emission spectra of **1a** (25  $\mu$ M) with varied glycerol fraction in THF/glycerol mixture



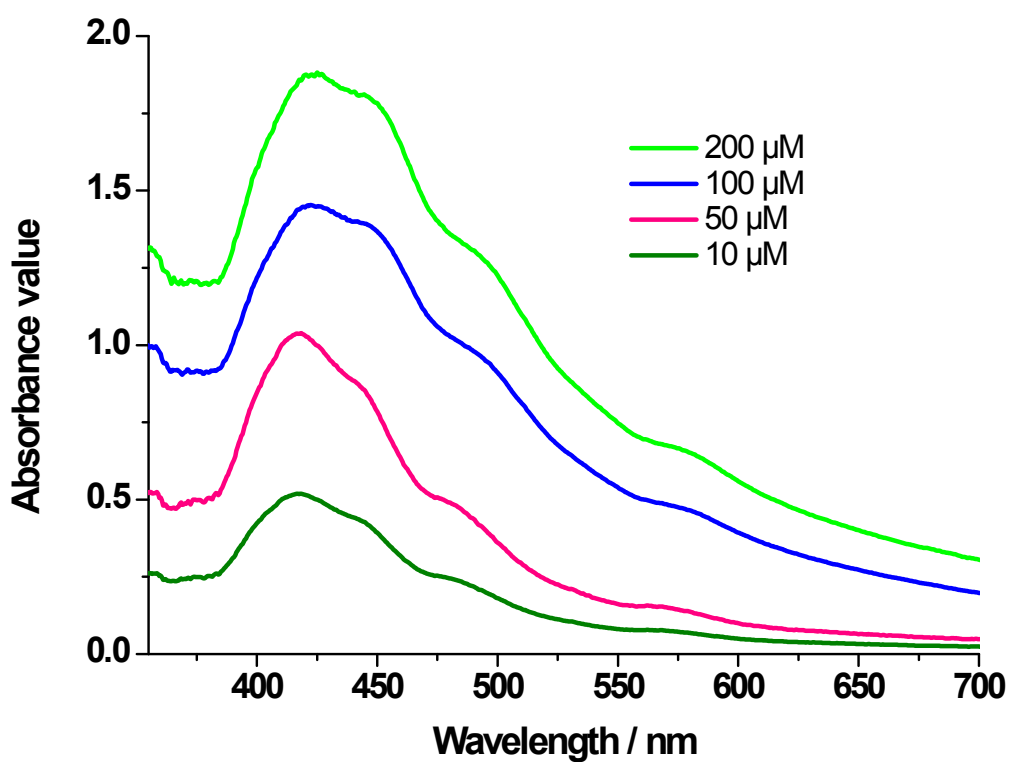
**Fig. S19** Emission spectra of **1b** (25  $\mu$ M) with varied glycerol fraction in THF/glycerol mixture



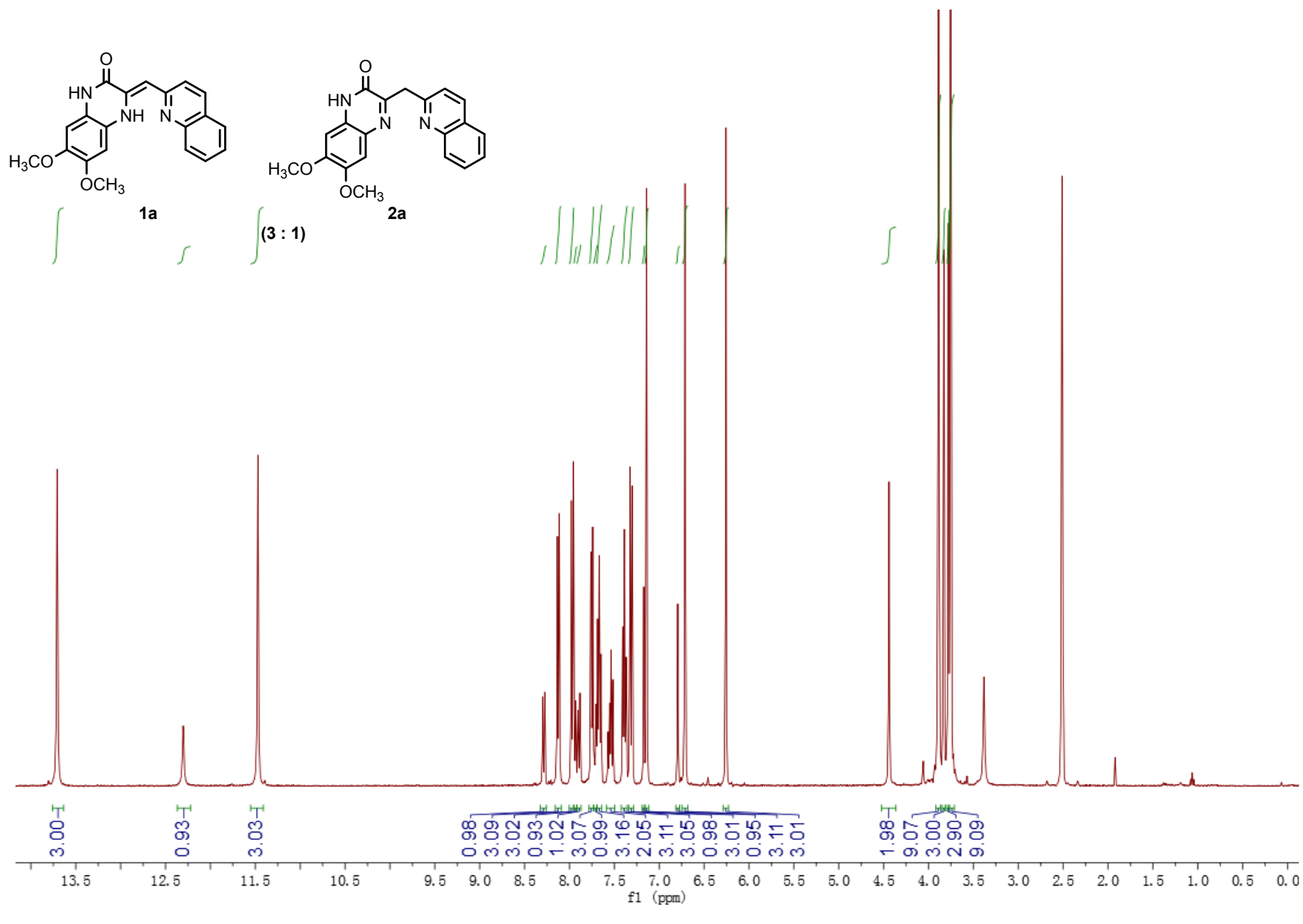
**Fig. S20** Emission spectra of **1d** (25 μM) with varied glycerol fraction in THF/glycerol mixture

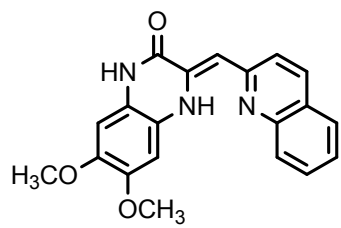


**Fig. S21** Absorption spectra of **1c** in THF solution with different concentration

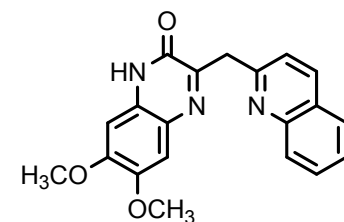


**Fig. 22** Absorption spectra of **1c** with different concentration in THF/H<sub>2</sub>O(1:9, v/v) mixture



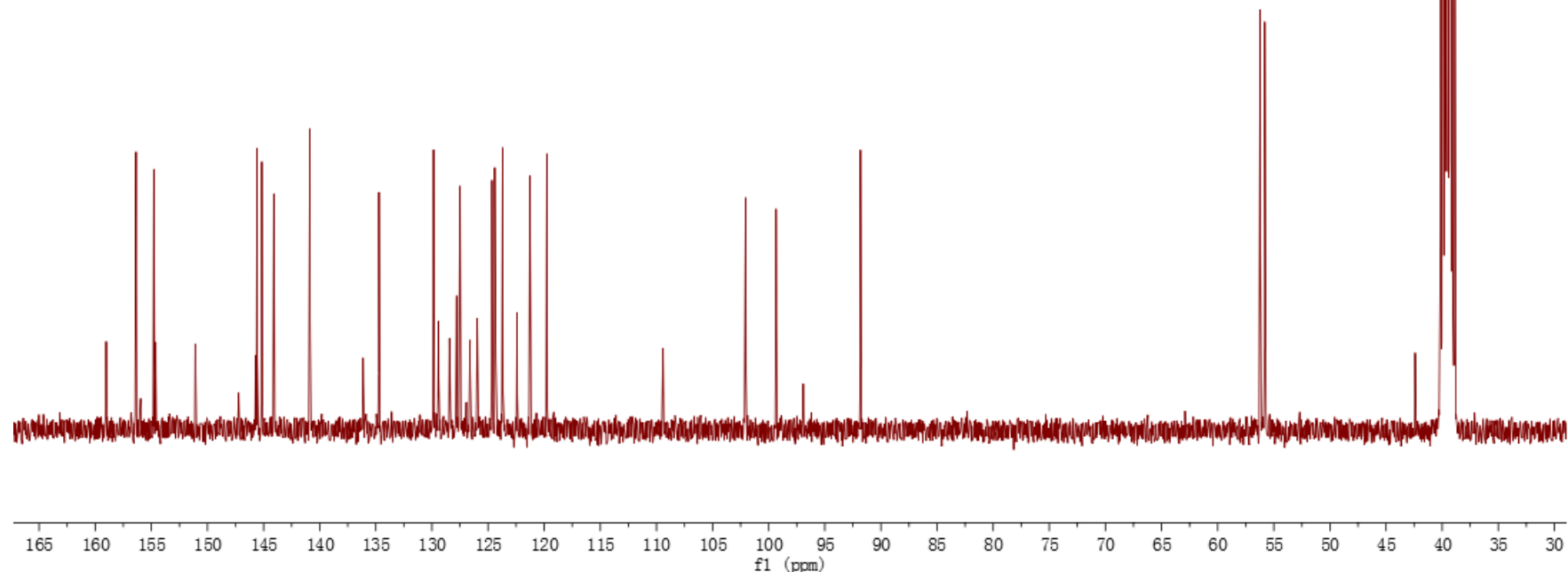


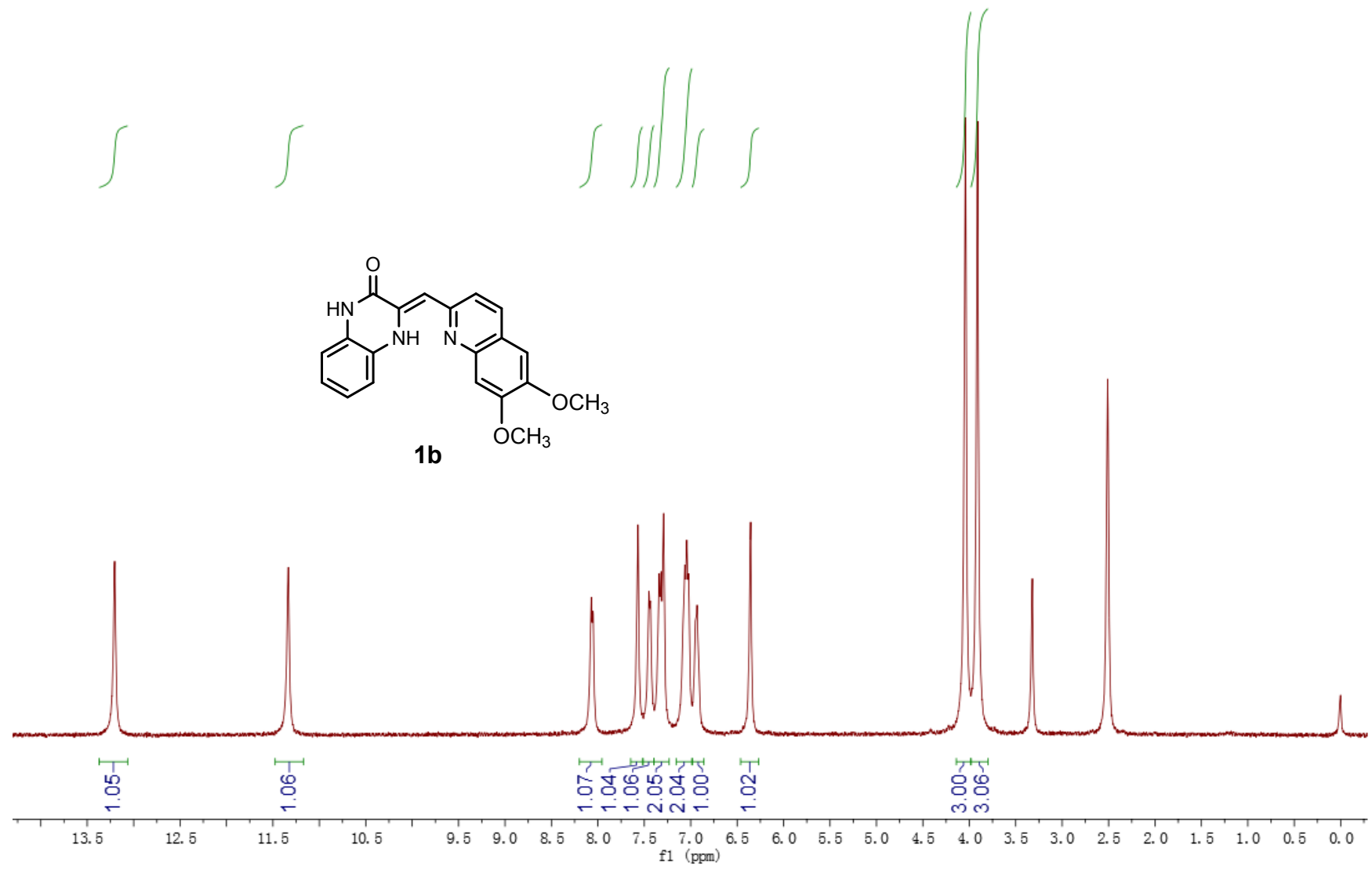
**1a**

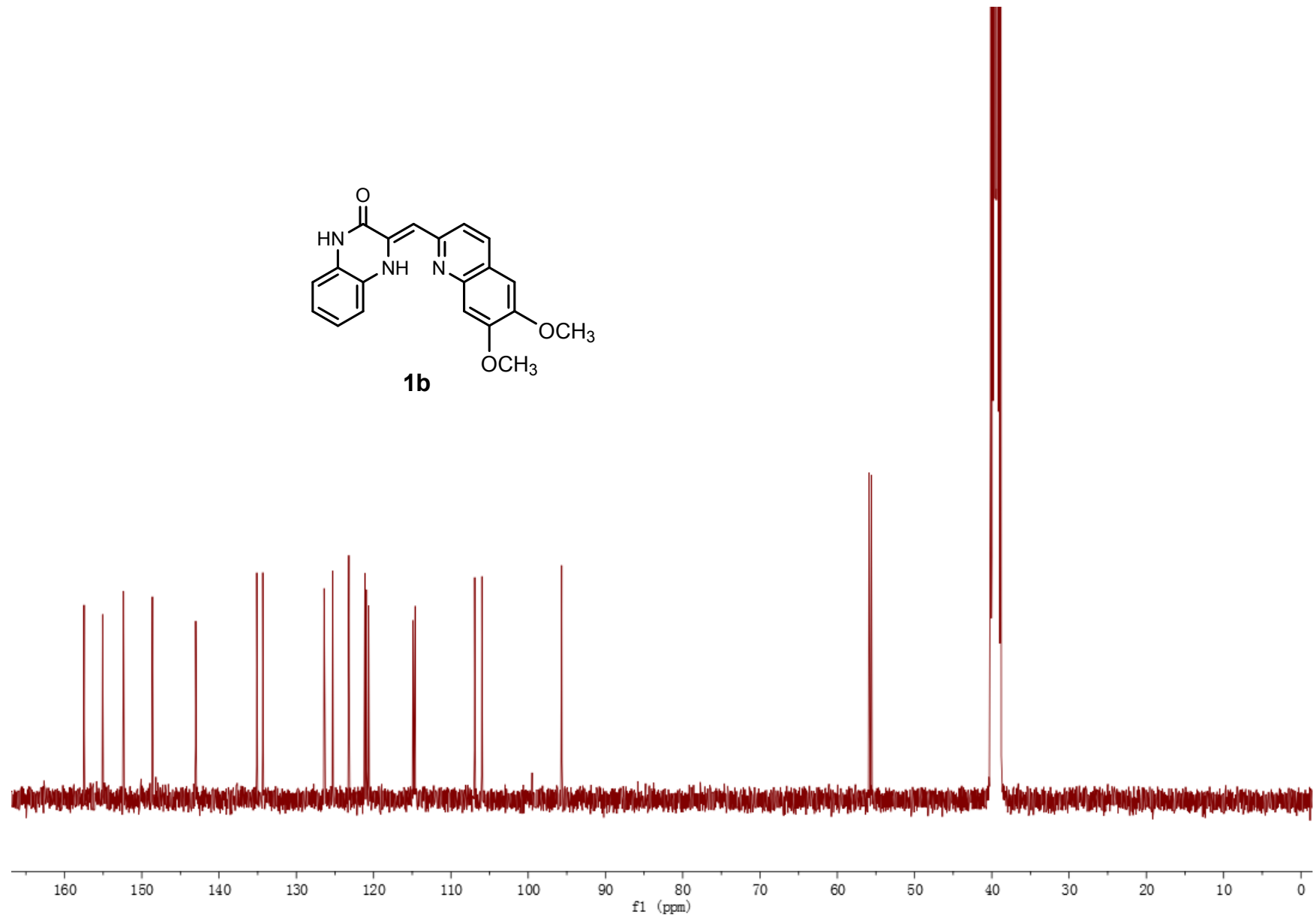
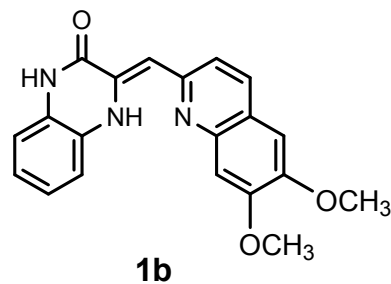


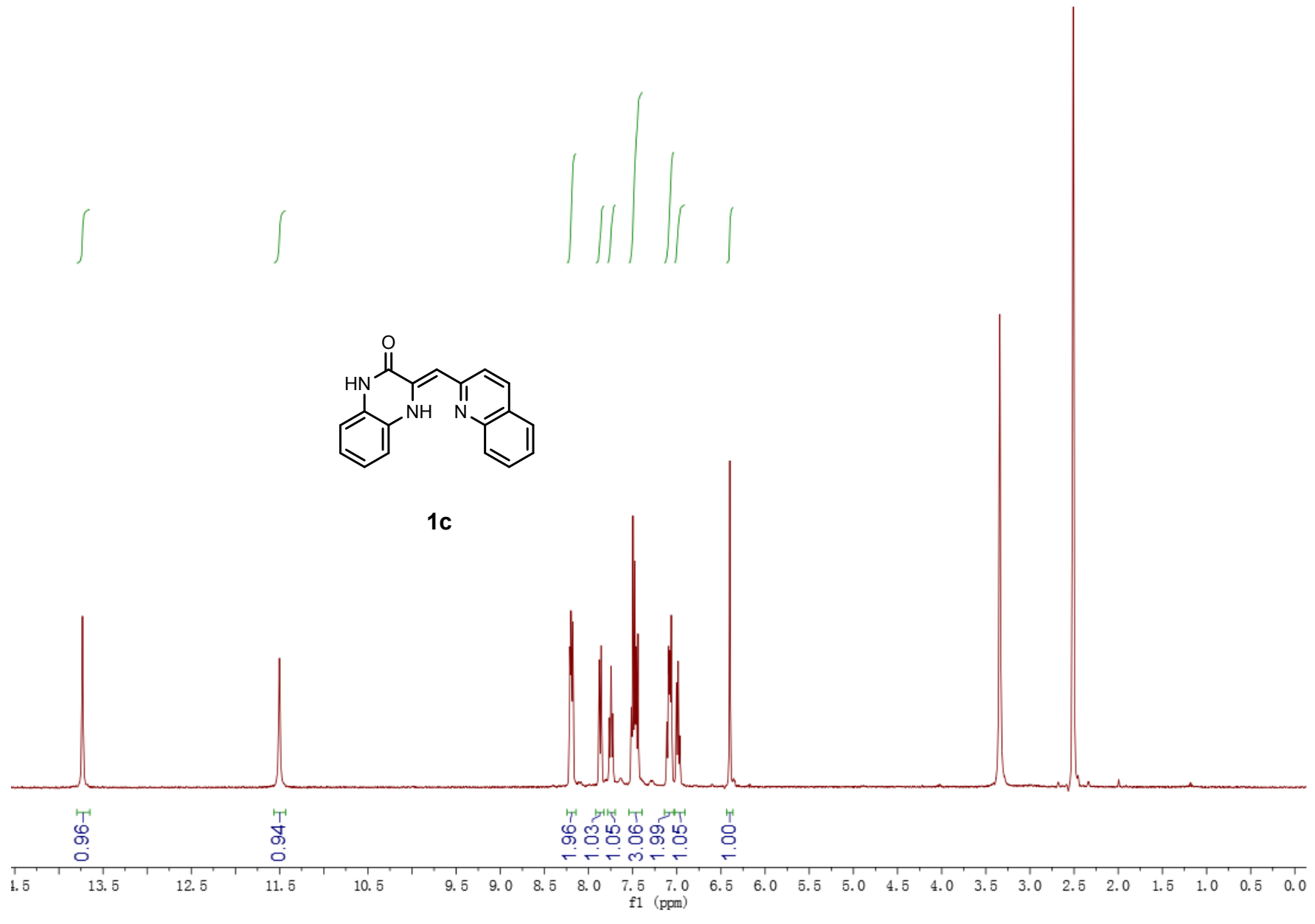
**2a**

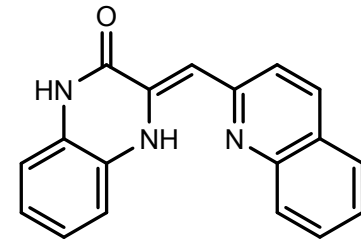
(3 : 1)



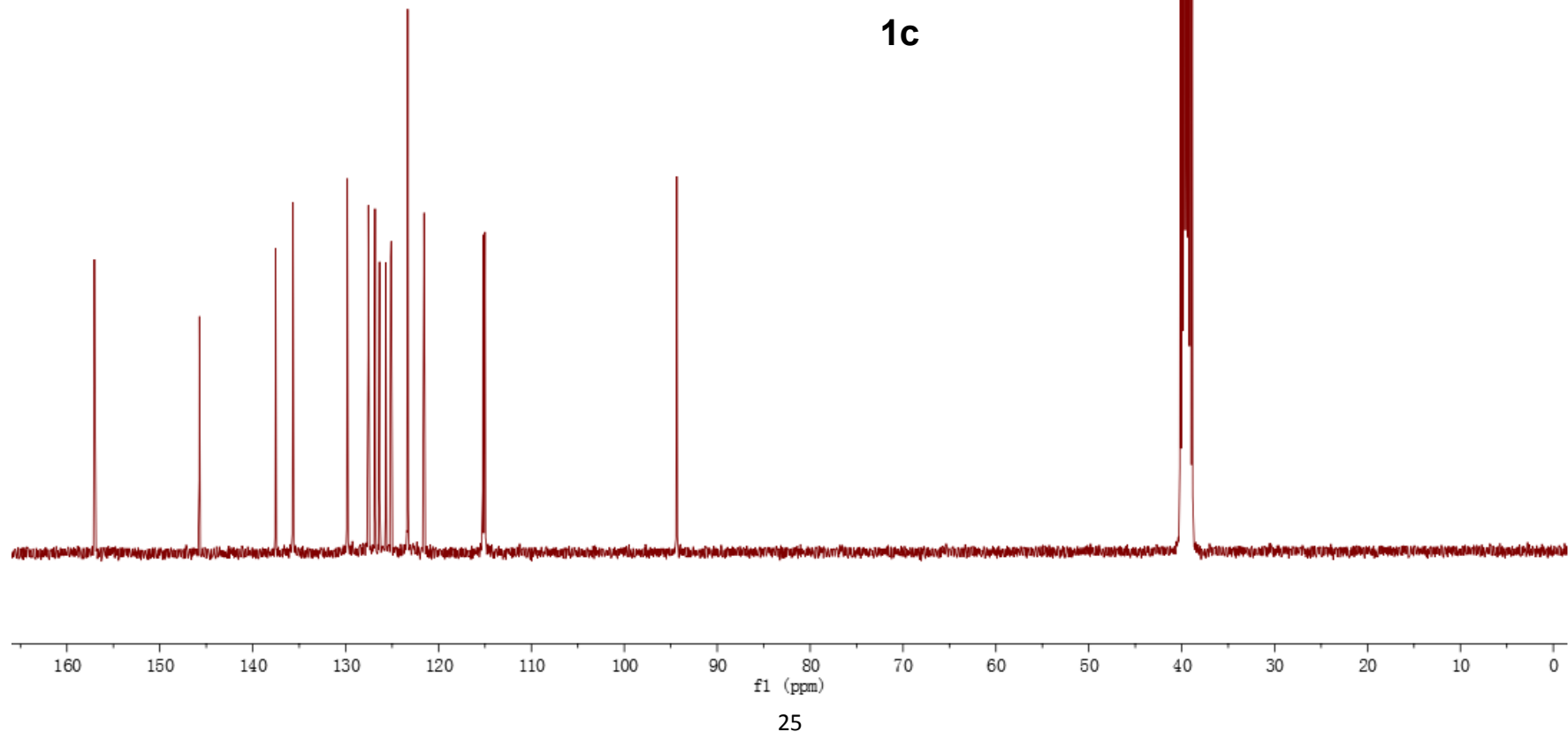


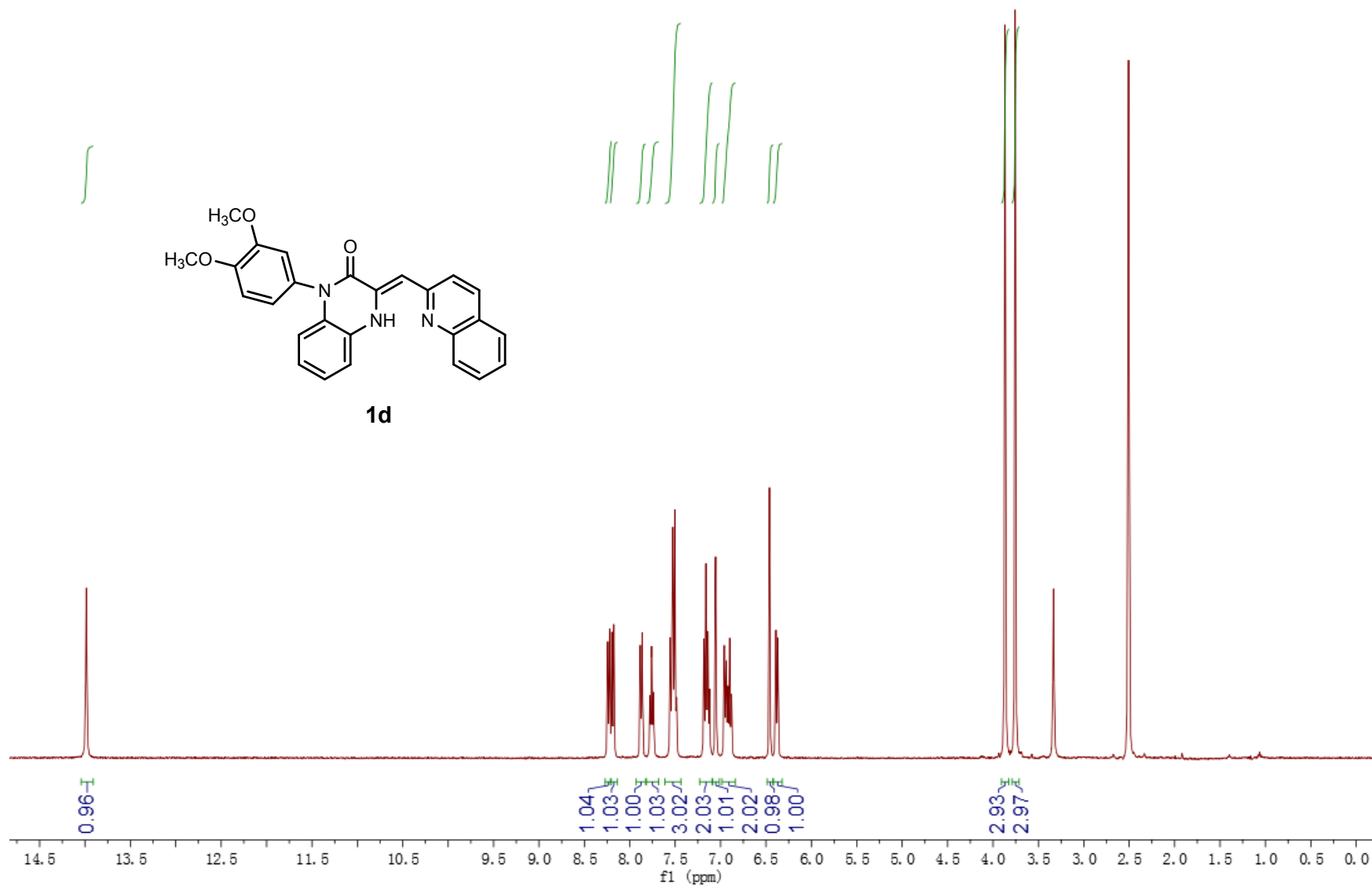


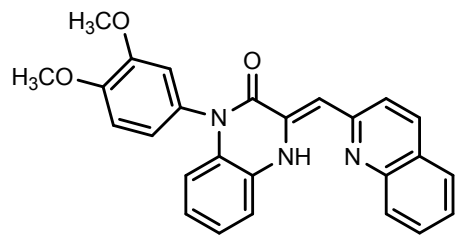




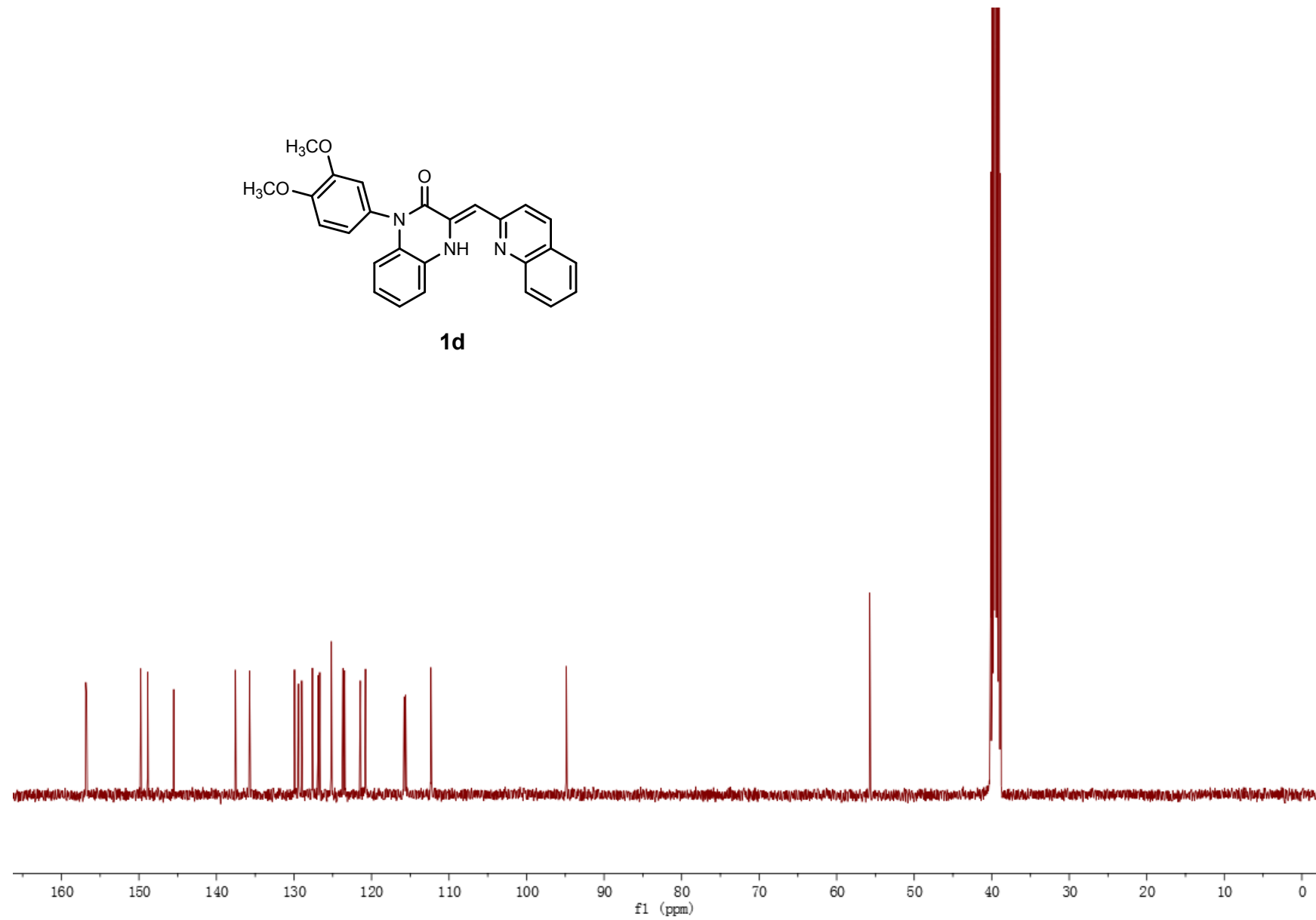
**1c**

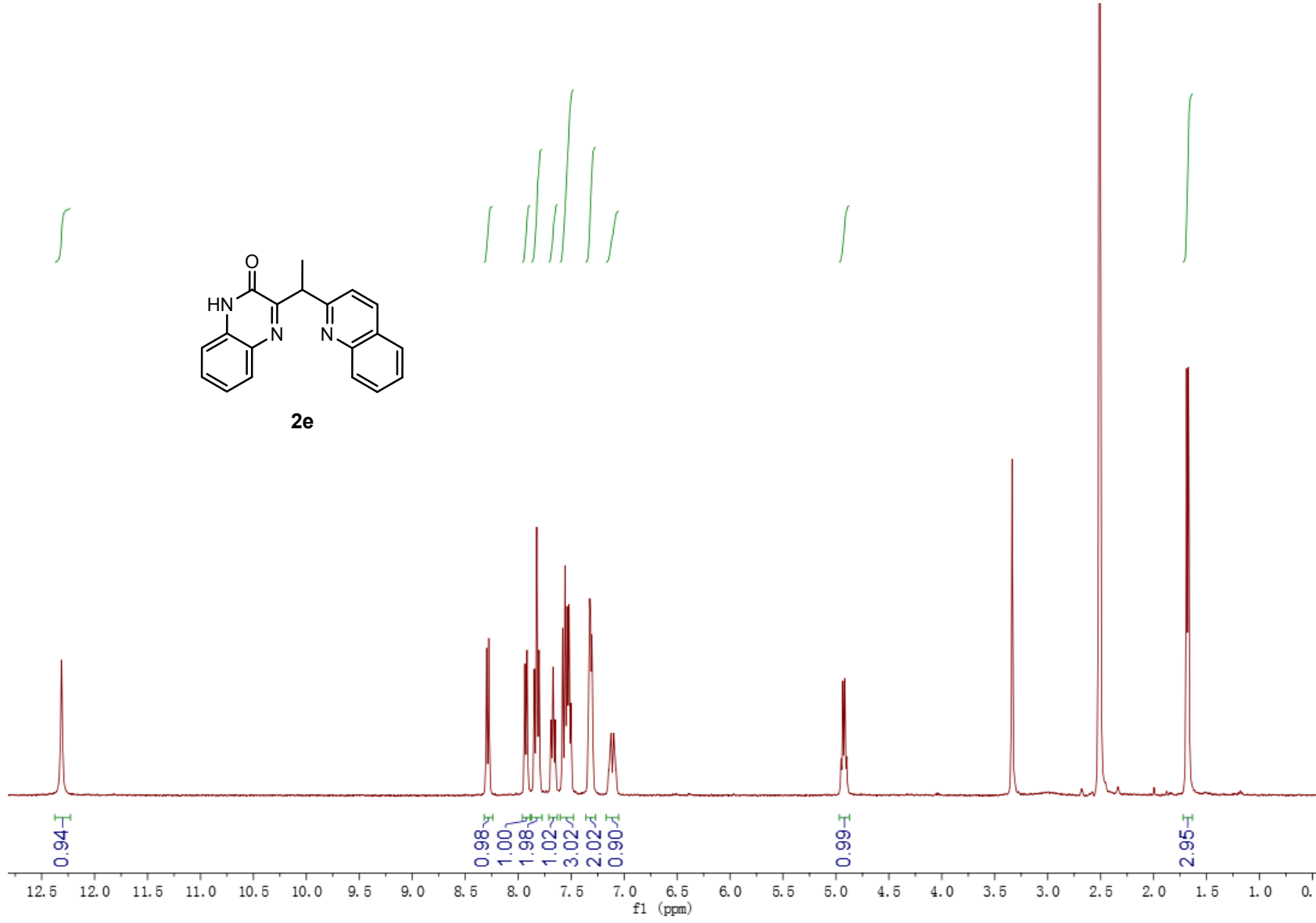


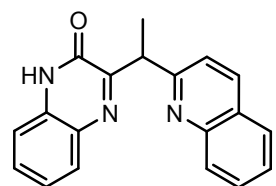




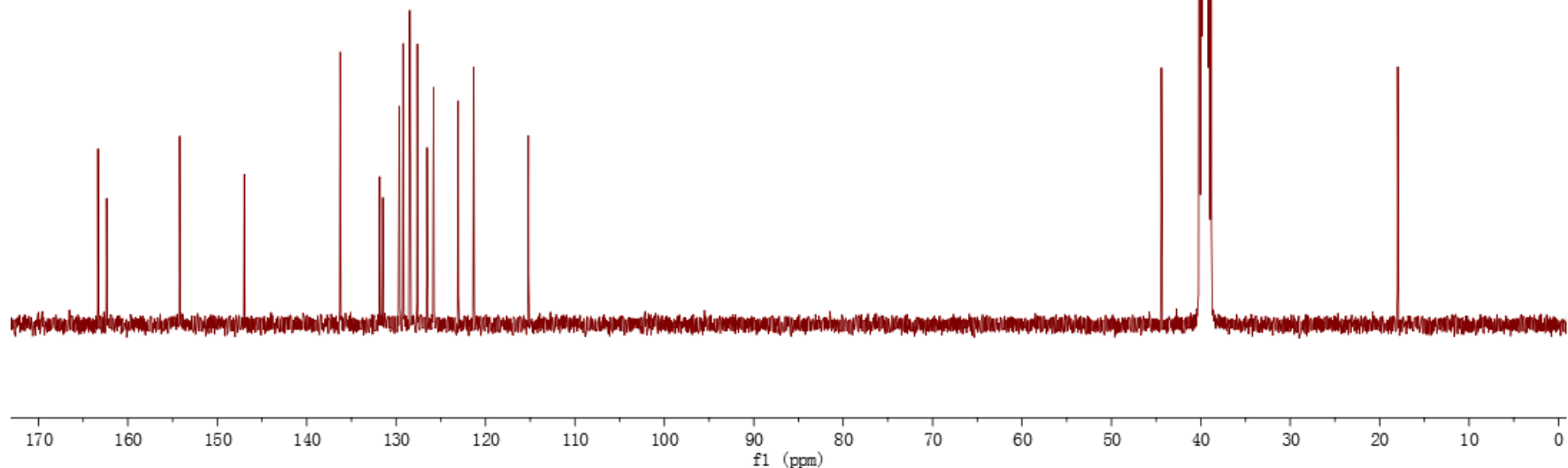
**1d**

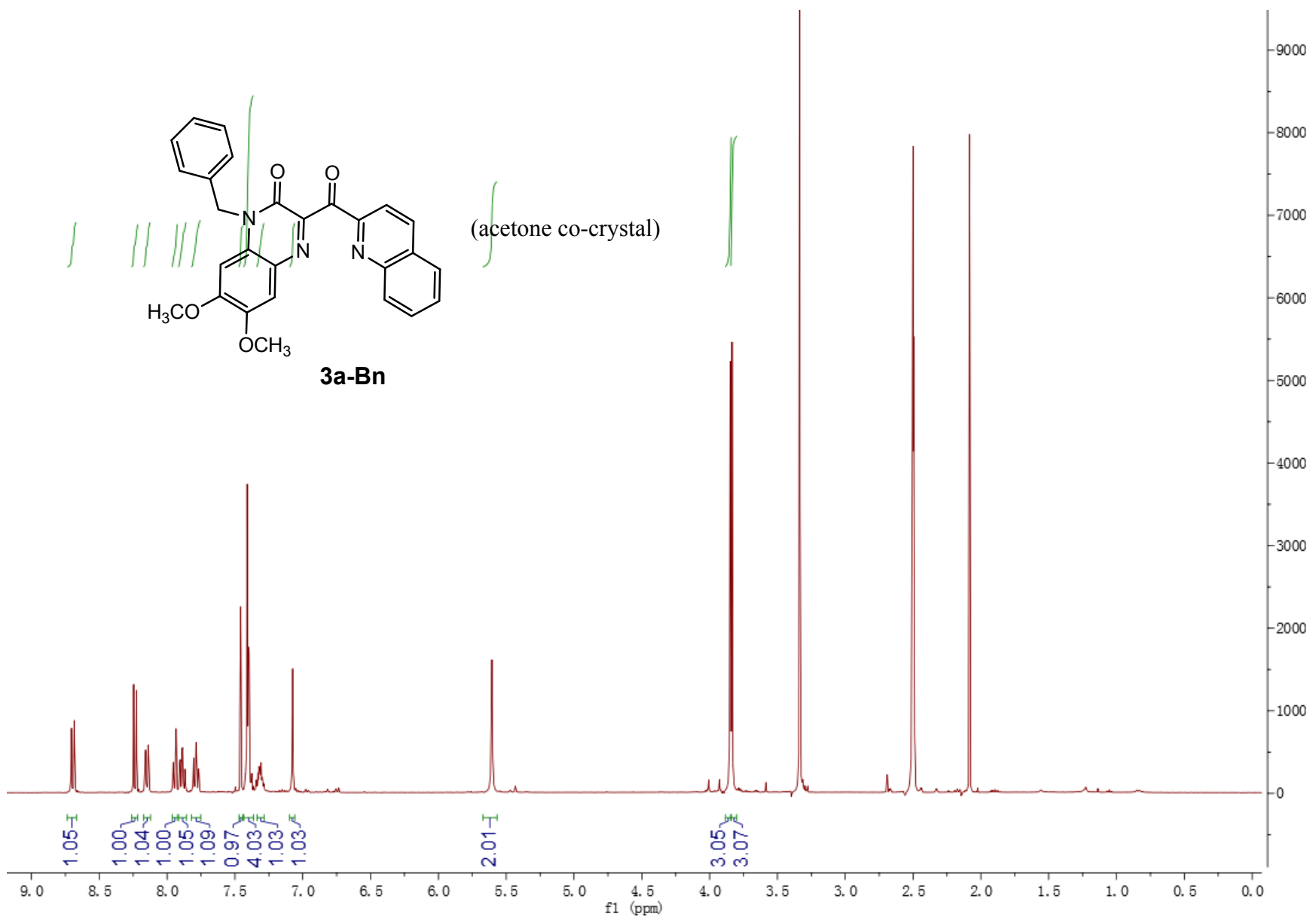


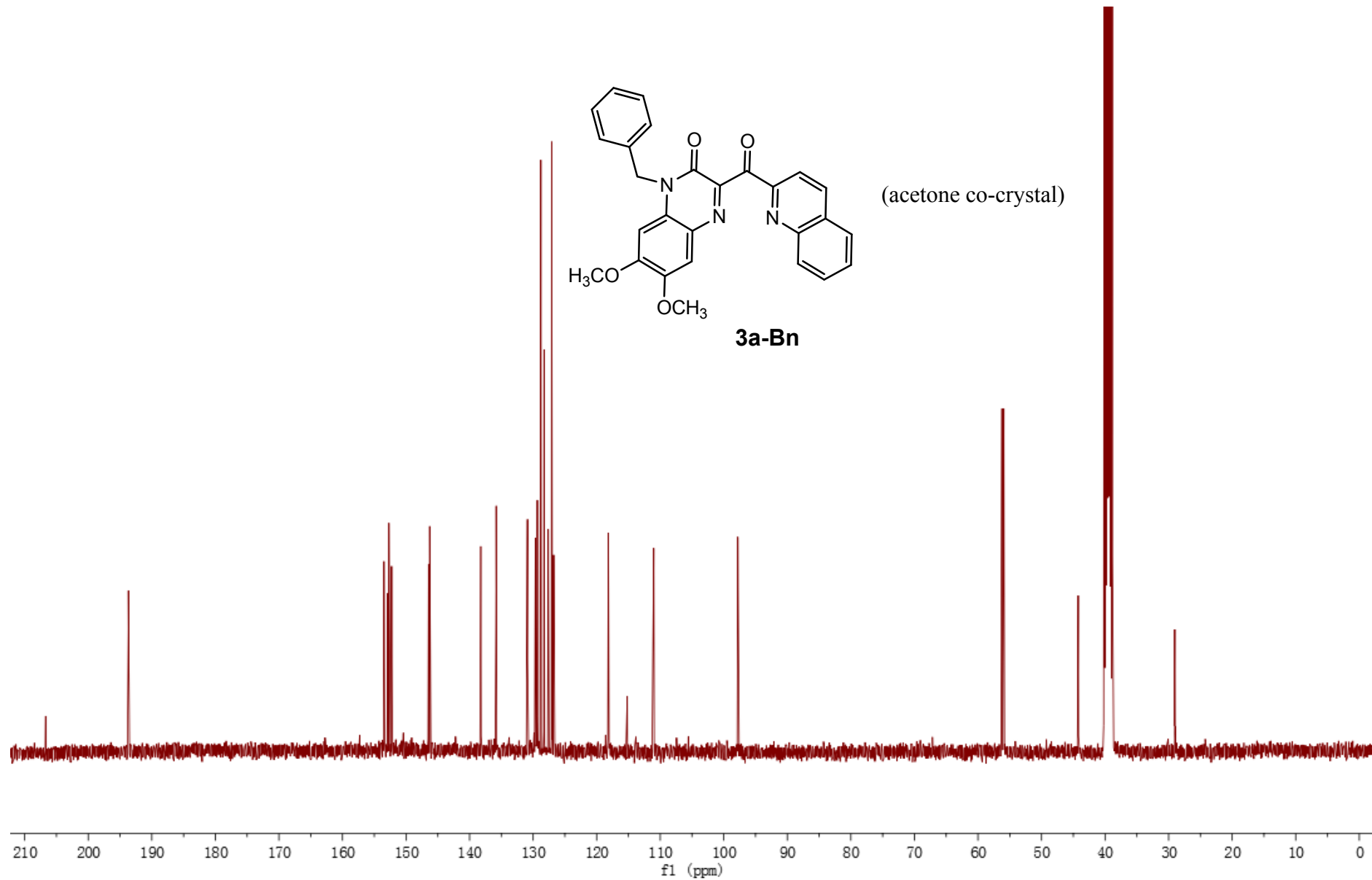


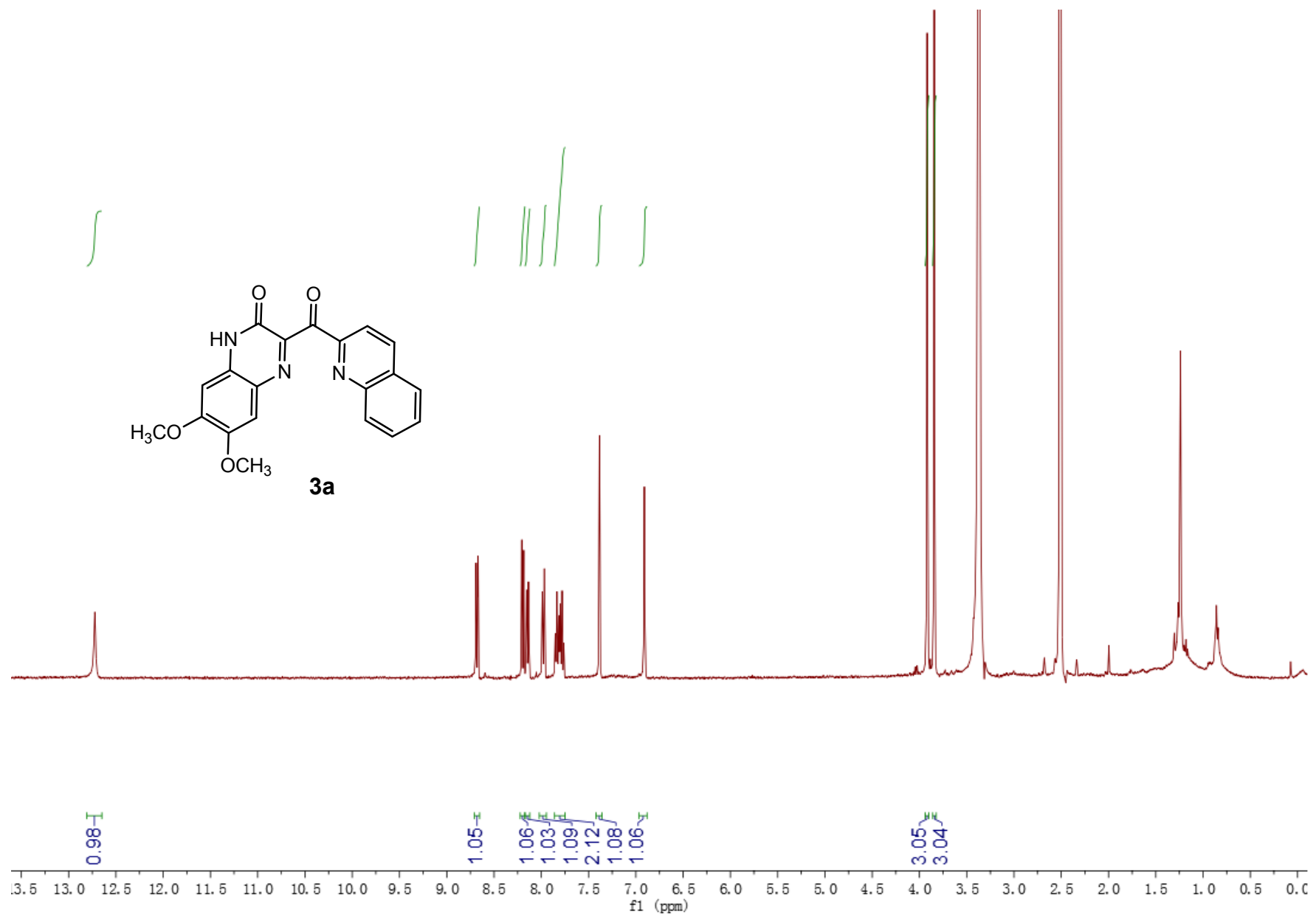


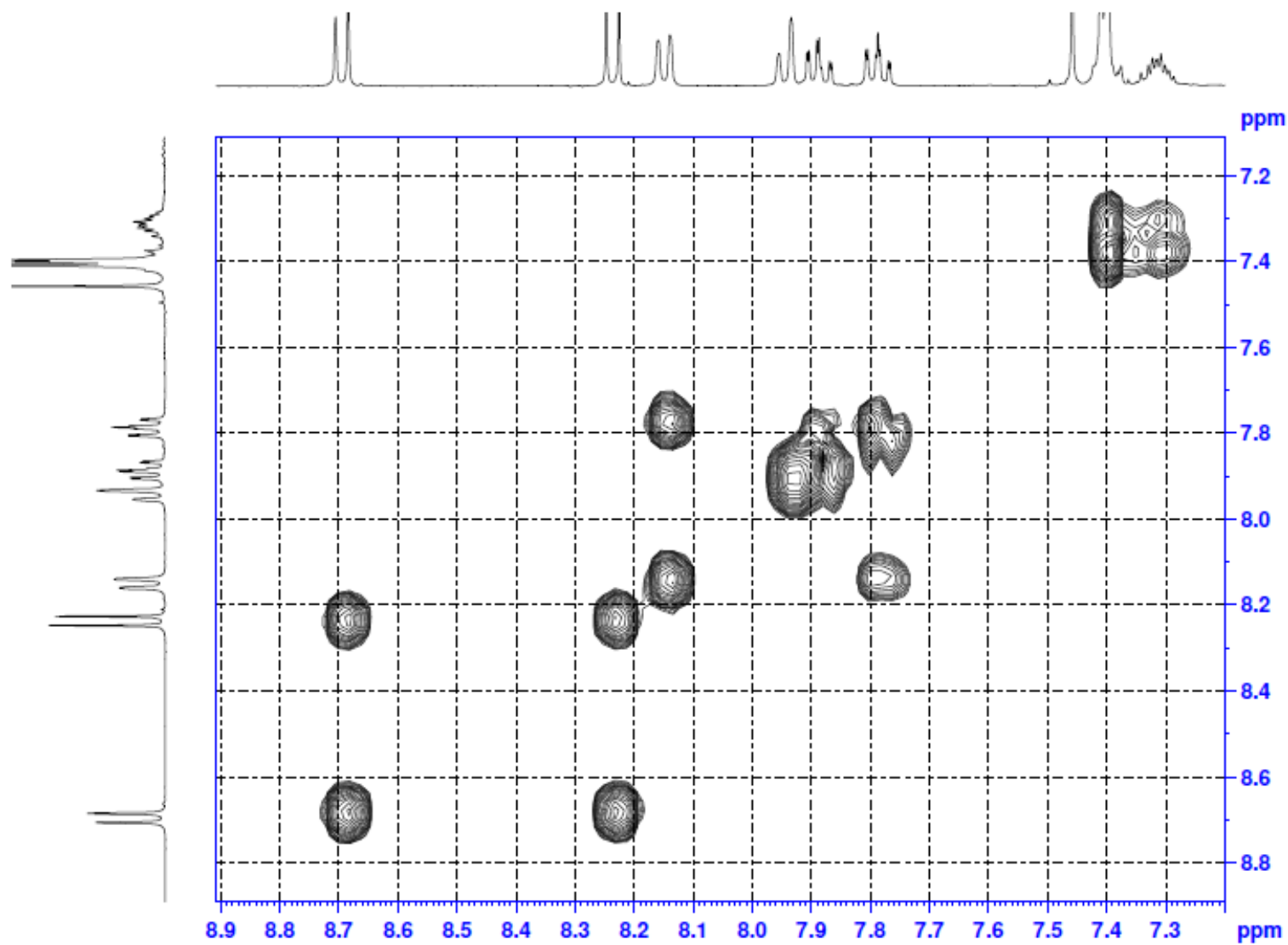
**2e**

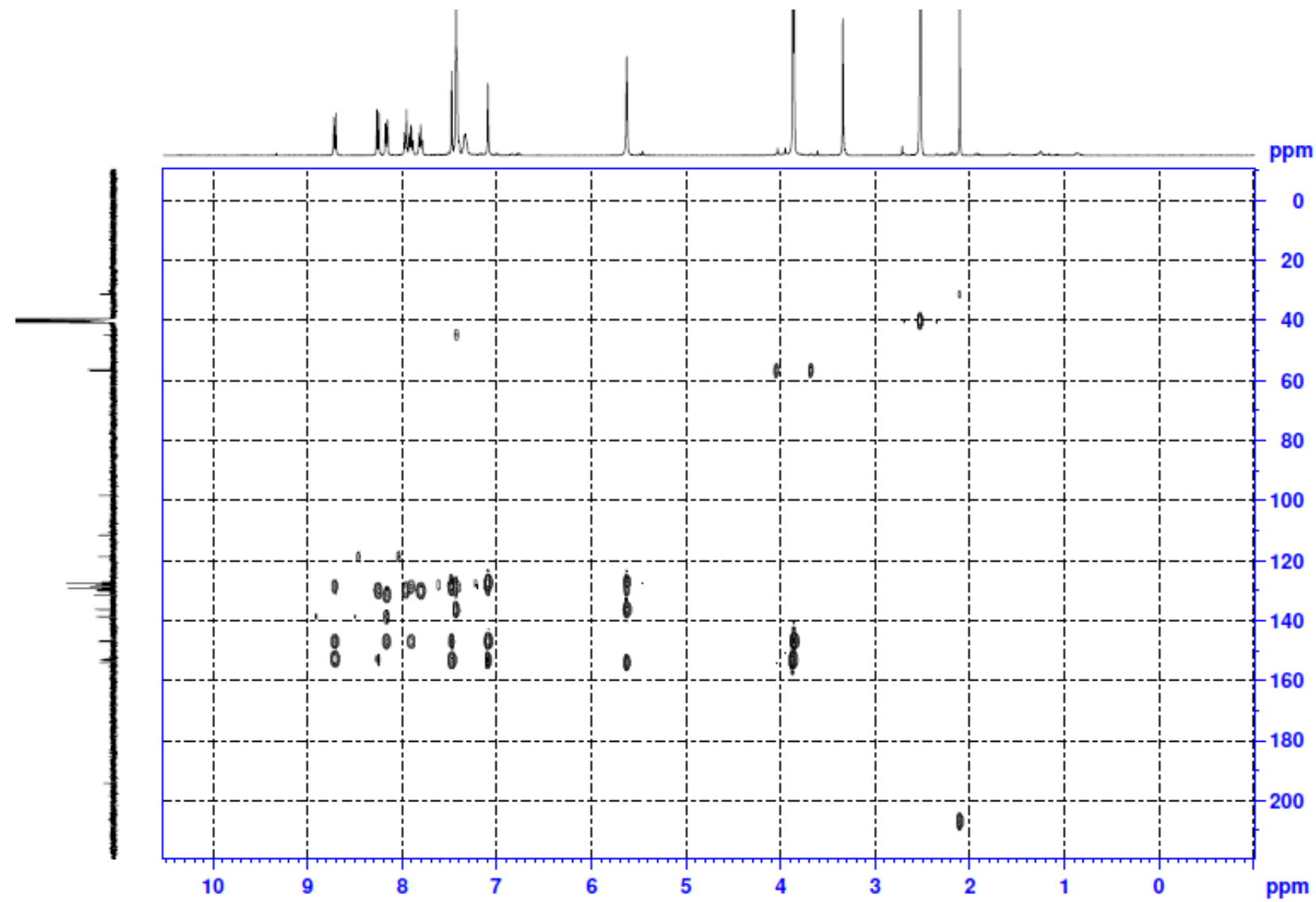


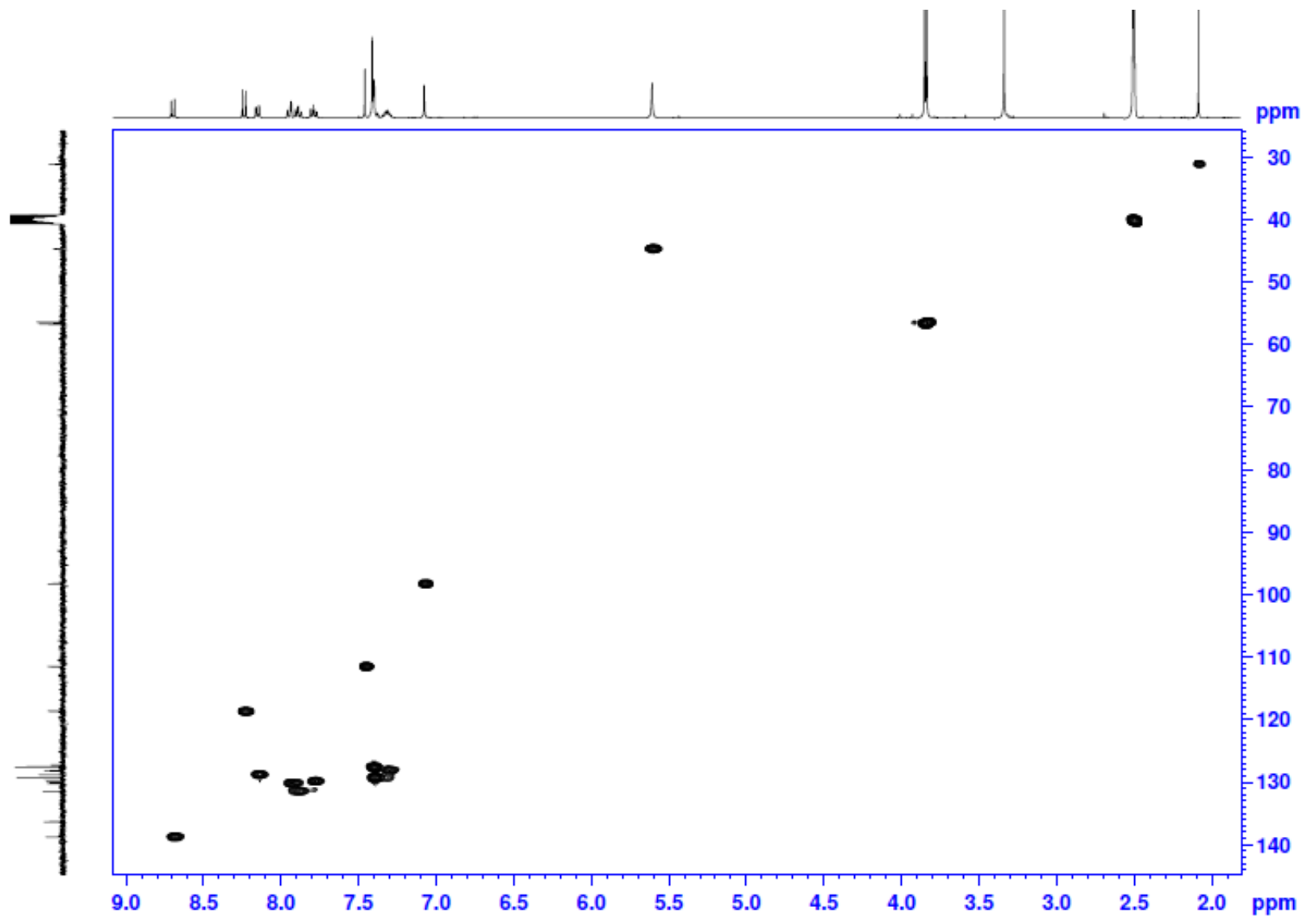


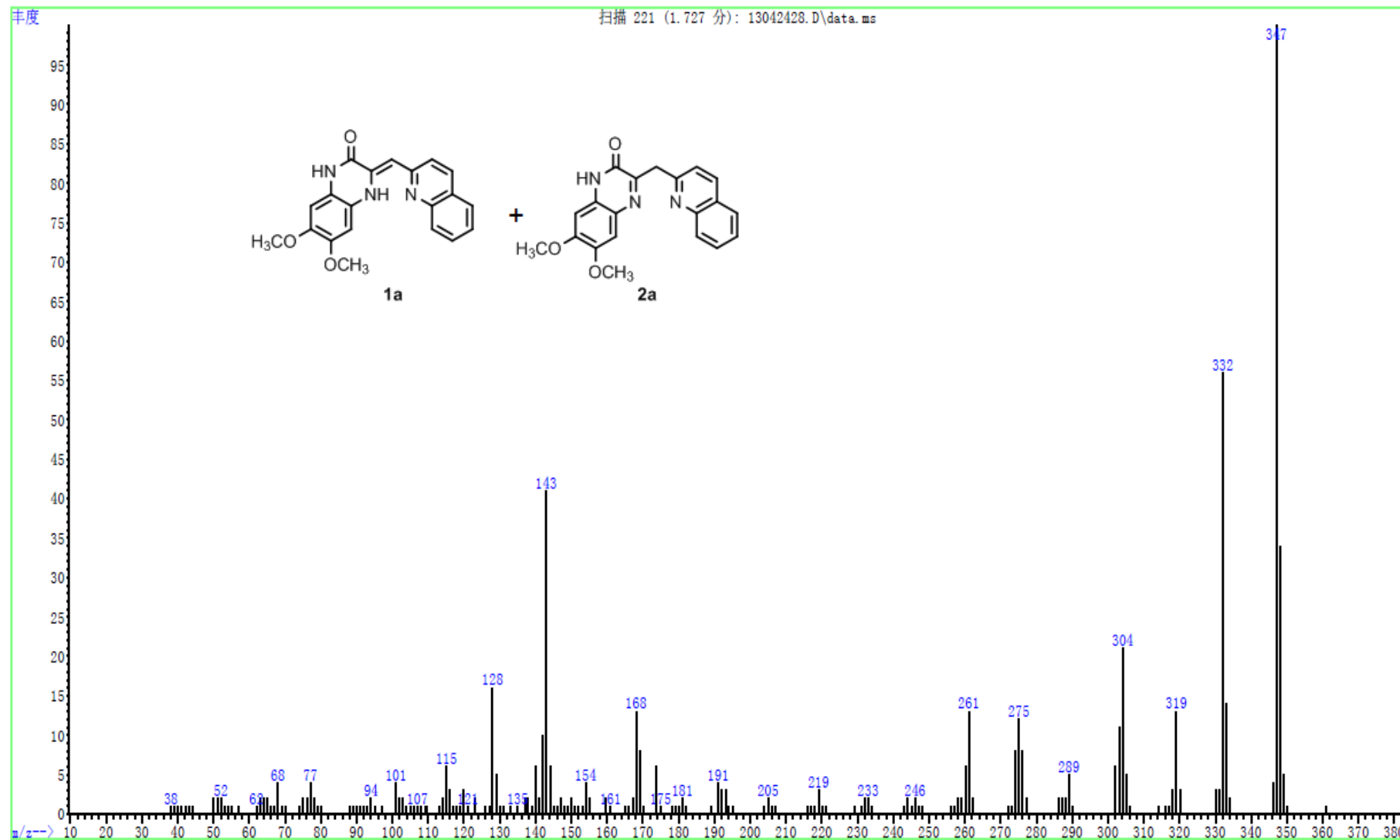


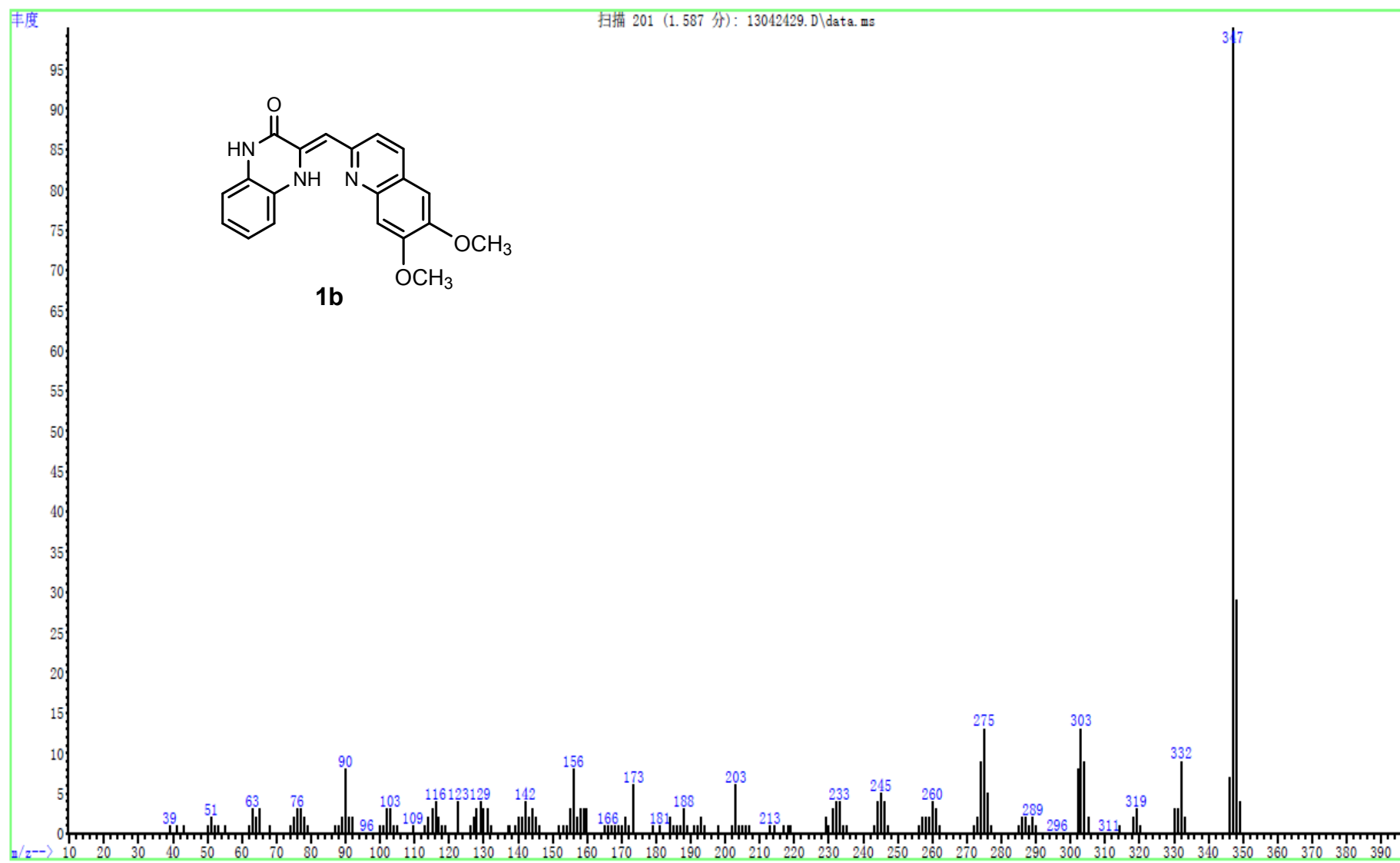


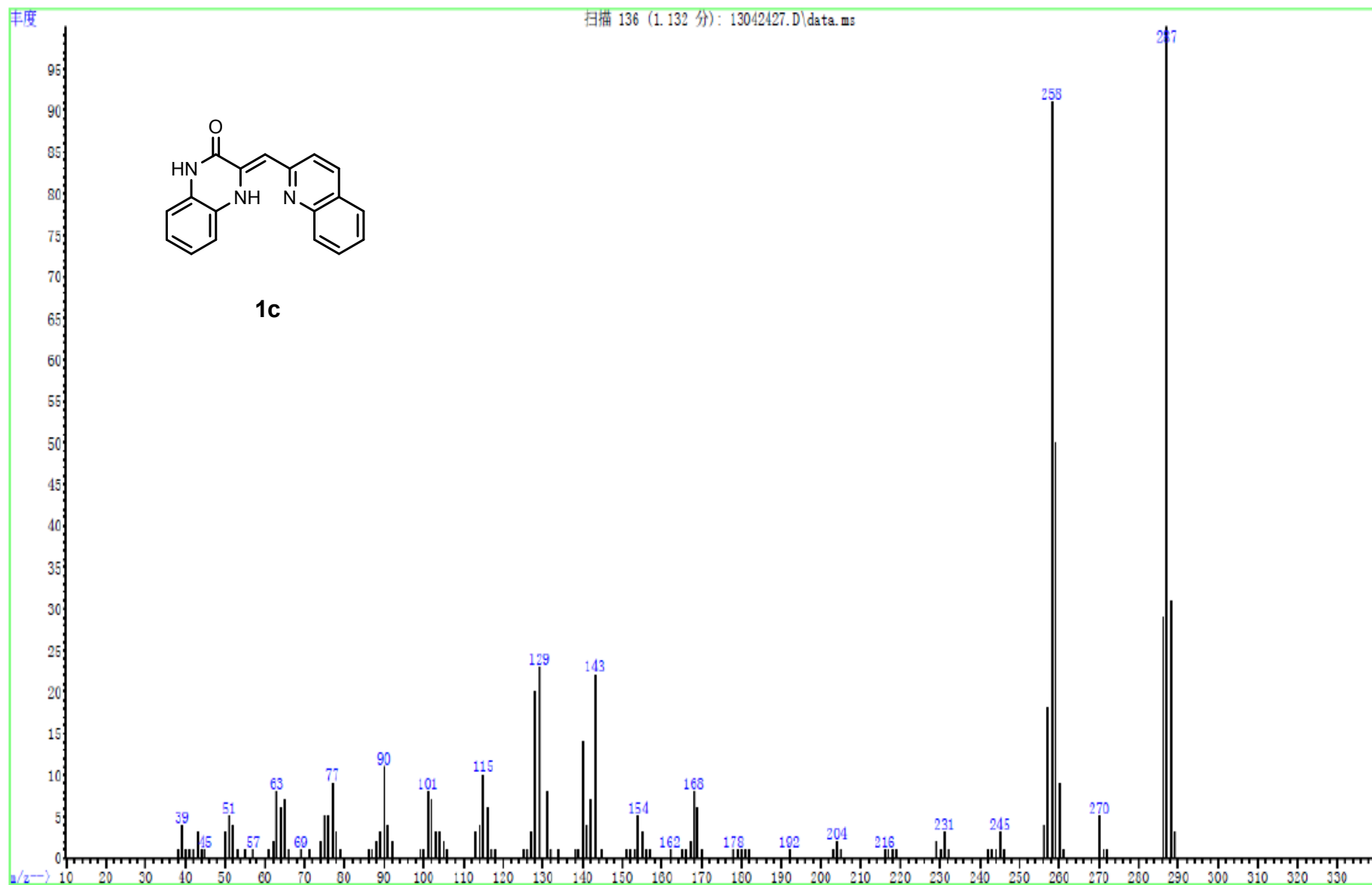


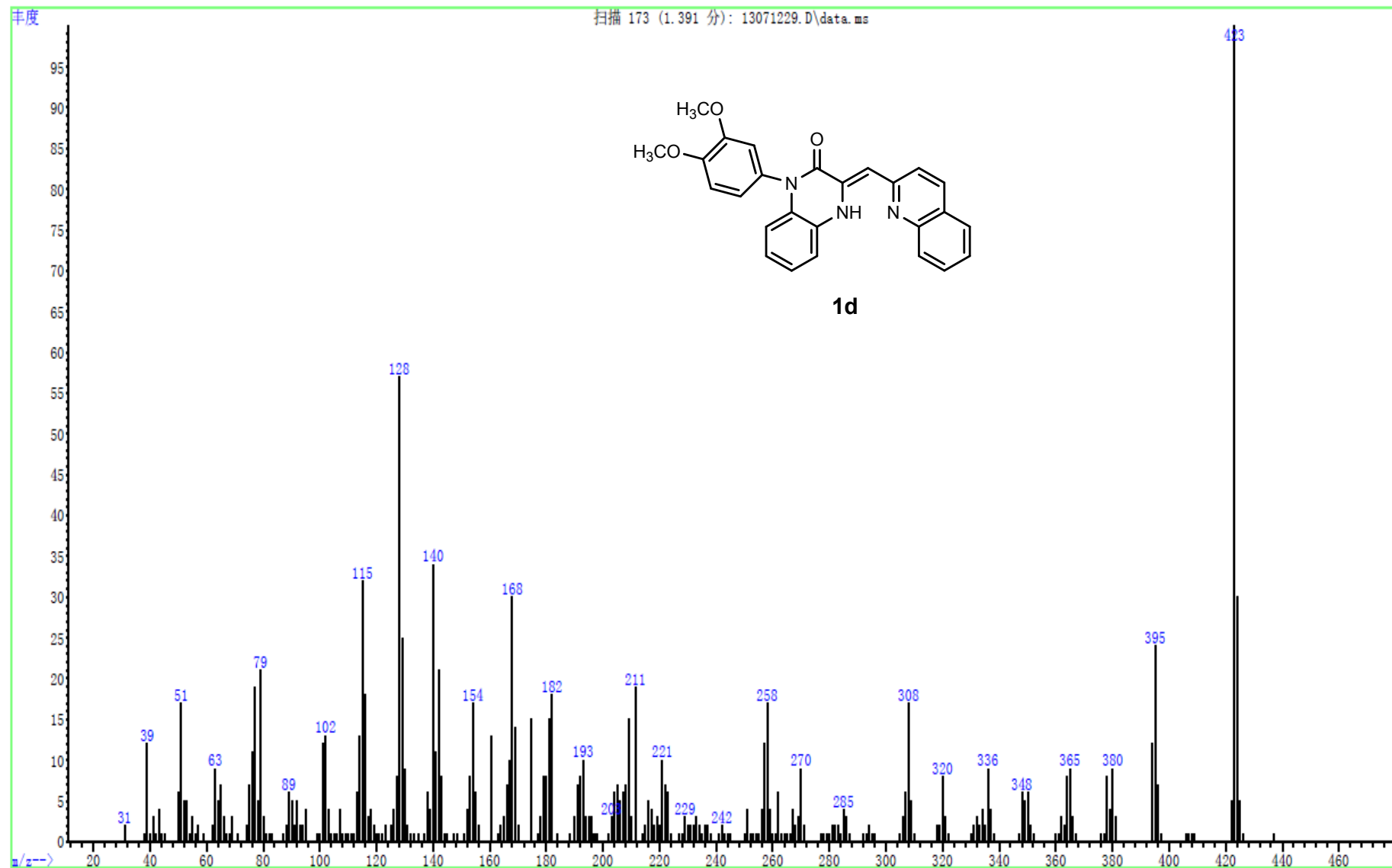


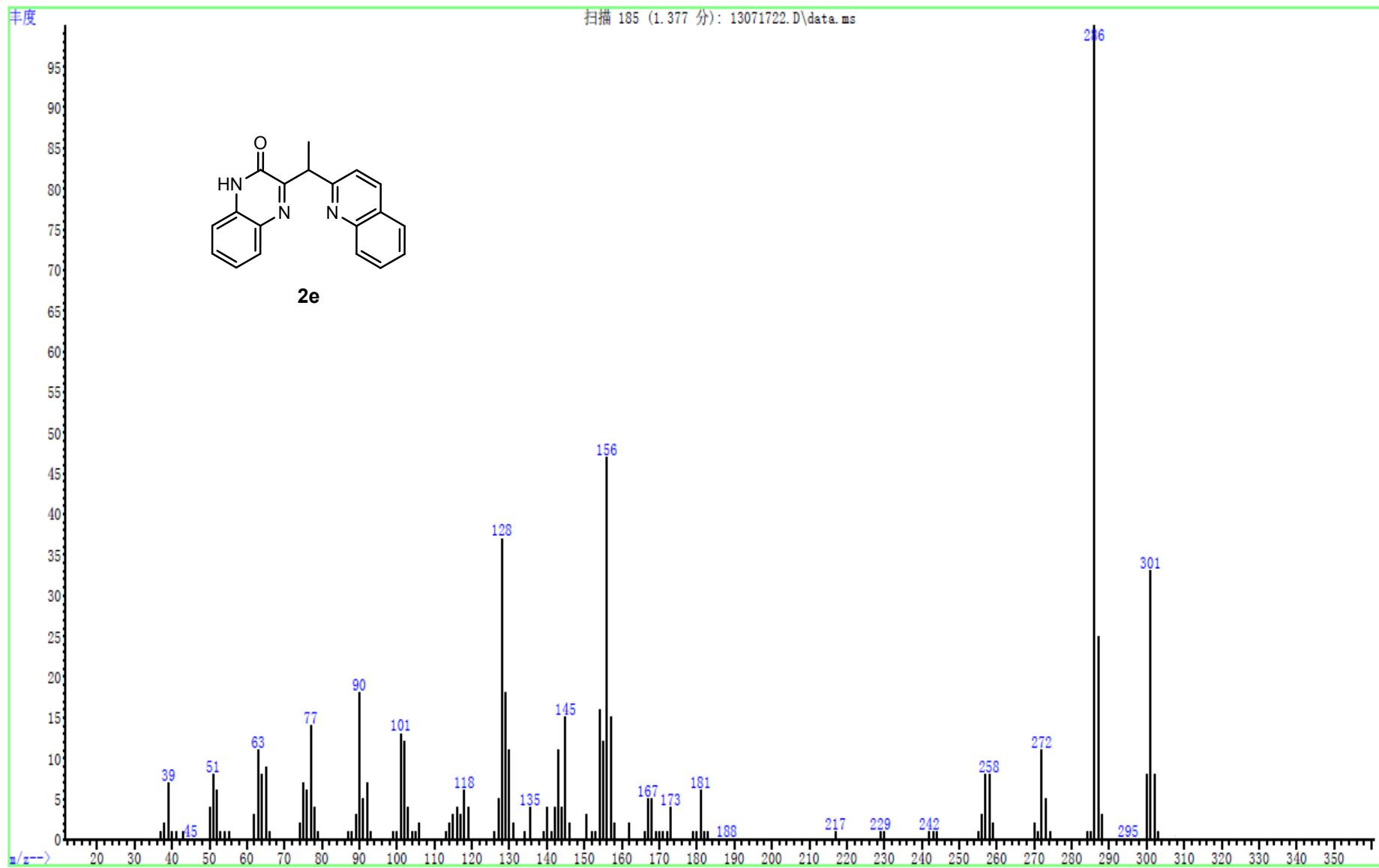


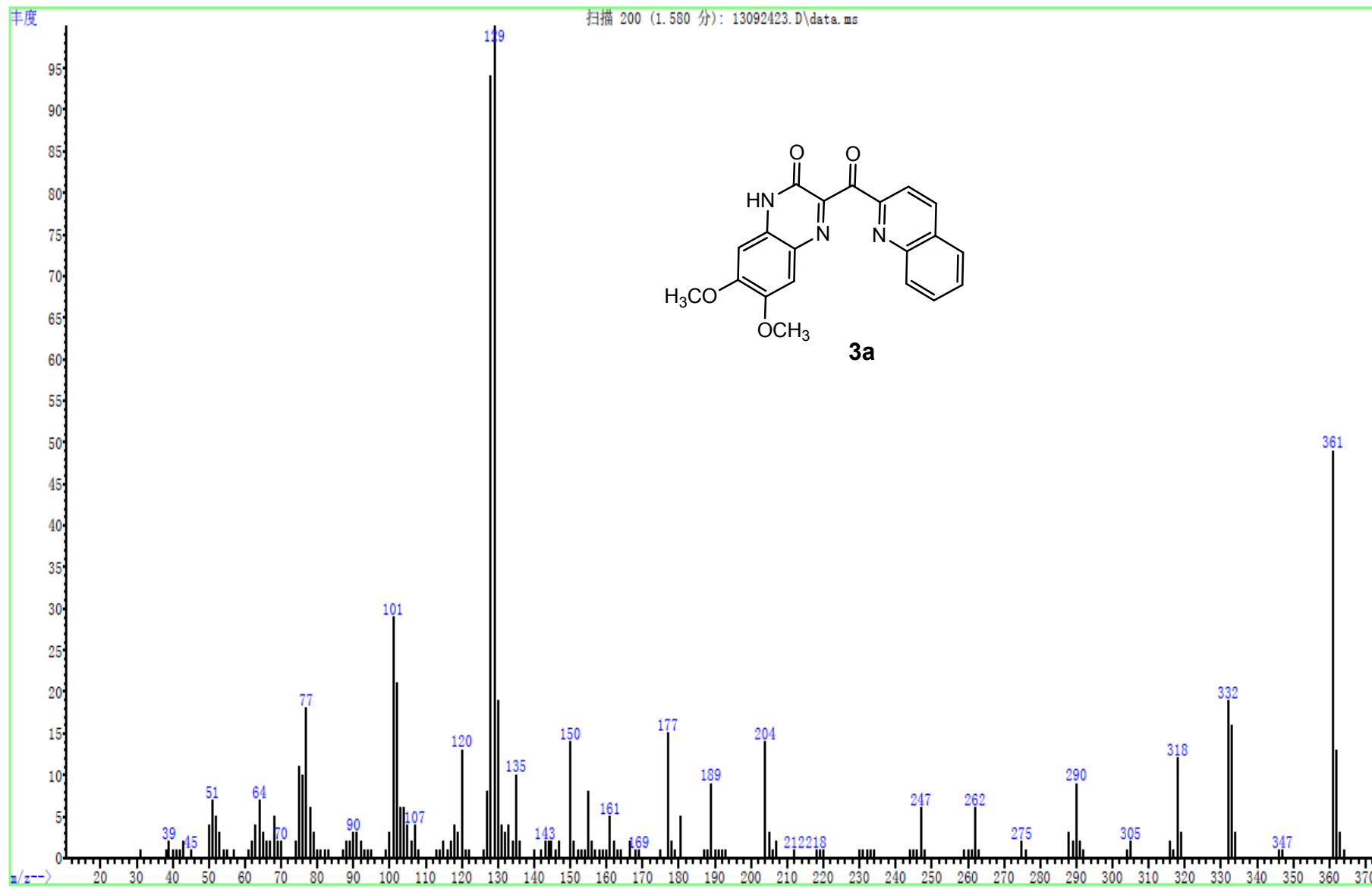


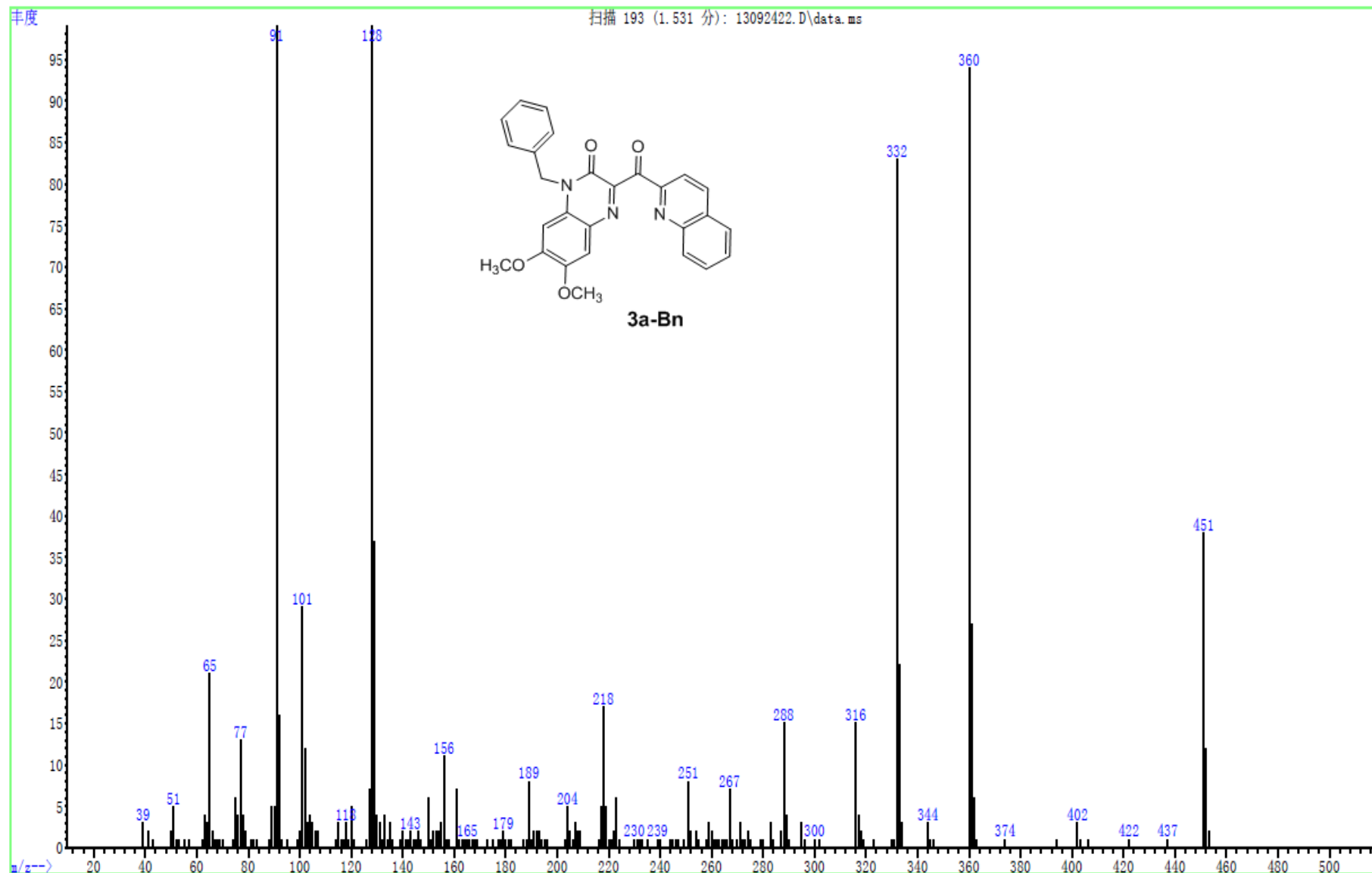












## References

- 1 (a) A. D. Becke, *J. Chem. Phys.*, 1993, **98**, 5648–5652; (b) C. Lee, W. Yang, R. G. Parr, *Phys. Rev. B*, 1988, **37**, 785–789.
- 2 M. J. Frisch, G. W. Trucks, H. B. Schlegel, G. E. Scuseria, M. A. Robb, J. R. Cheeseman, G. Scalmani, V. Barone, B. Mennucci, G. A. Petersson, H. Nakatsuji, M. Caricato, X. Li, H. P. Hratchian, A. F. Izmaylov, J. Bloino, G. Zheng, J. L. Sonnenberg, M. Hada, M. Ehara, K. Toyota, R. Fukuda, J. Hasegawa, M. Ishida, T. Nakajima, Y. Honda, O. Kitao, H. Nakai, T. Vreven, J. A. Montgomery, Jr., J. E. Peralta, F. Ogliaro, M. Bearpark, J. J. Heyd, E. Brothers, K. N. Kudin, V. N. Staroverov, R. Kobayashi, J. Normand, K. Raghavachari, A. Rendell, J. C. Burant, S. S. Iyengar, J. Tomasi, M. Cossi, N. Rega, J. M. Millam, M. Klene, J. E. Knox, J. B. Cross, V. Bakken, C. Adamo, J. Jaramillo, R. Gomperts, R. E. Stratmann, O. Yazyev, A. J. Austin, R. Cammi, C. Pomelli, J. W. Ochterski, R. L. Martin, K. Morokuma, V. G. Zakrzewski, G. A. Voth, P. Salvador, J. J. Dannenberg, S. Dapprich, A. D. Daniels, O. Farkas, J. B. Foresman, J. V. Ortiz, J. Cioslowski, D. J. Fox, Gaussian 09, Revision A.02, Gaussian, Inc., Wallingford CT, 2009.
- 3 (a) M. Cossi, N. Rega, G. Scalmani, V. Barone, *J. Comput. Chem.*, 2003, **24**, 669–681; (b) N. M. O’Boyle, A. L. Tenderhol K. M. Langner, *J. Comput. Chem.*, 2008, **29**, 839–845.